DOI: 10.1002/ ((please add manuscript number))

Article type: Progress Report

When 2D materials meet molecules: opportunities and challenges of hybrid organic/inorganic van der Waals heterostructures.

*Marco Gobbi, Emanuele Orgiu, Paolo Samorì**

Dr. M. Gobbi, Prof. E. Orgiu, Prof. P. Samorì
University of Strasbourg, CNRS, ISIS UMR 7006, 8 allée Gaspard Monge, F-67000 Strasbourg, France.

Dr. M. Gobbi
Present address: Centro de Fisica de Materiales, Paseo Manuel de Lardizabal, 5 – E-20018 Donostia – San Sebastián (Gipzukoa) – Spain

Prof. E. Orgiu
Present address: Institut national de la recherche scientifique (INRS), EMT Center, 1650 Boulevard Lionel-Boulet, J3X 1S2 Varennes, Quebec, Canada

E-mail: samori@unistra.fr

Keywords: 2D materials, devices, molecular self-assembly, van der Waals heterostructures, functional materials.

Abstract

Van der Waals heterostructures, composed of vertically stacked inorganic 2D materials, represent an ideal platform to demonstrate novel device architectures and to fabricate on-demand materials. The incorporation of organic molecules within these systems holds an immense potential, since while nature offers a finite number of 2D materials, an almost unlimited variety of molecules can be designed and synthesized with predictable functionalities. The scope of this work is to emphasize the possibilities offered by systems in which continuous molecular layers are interfaced with inorganic 2D materials to form hybrid organic/inorganic van der Waals heterostructures. Similarly to their inorganic counterpart, the hybrid structures have been exploited to put forward novel device architectures, such as antiambipolar transistors and barristors. Moreover, specific molecular groups can be employed to modify intrinsic properties and confer new capabilities to 2D materials. In particular, we will highlight how molecular self-assembly at the surface of 2D materials can be mastered to achieve precise control over position and density of (molecular) functional groups, paving the way for a new class of hybrid functional materials whose final properties can be selected by careful molecular design.

1. Introduction

The isolation of single layers of graphene[1] relies on the peculiar crystal structure of graphite, in which in-plane covalently bridged crystalline networks of carbon atoms are held together by out-of-plane inter-layer weak van der Waals (vdW) forces. A similar layered structure is encountered in nature in a variety of compounds, including boron nitride and the wide classes of transition metal dichalcogenides (TMDCs) and X-enes, to name a few. In analogy to graphite, several of such layered materials can be exfoliated to the single- or few- layer limit,[2–6] constituting the foundation for a new class of materials, i.e. two-dimensional materials (2DMs).[7,8]

All the constituents of the 2DM family are characterized by ultra-high surface sensitivity, determined by the presence of two exposed surfaces without a bulk separation. Apart from sharing this property, 2DMs feature a wide range of diverse electronic, optical and magnetic properties arising from the different chemical composition and crystal structure of the in-plane covalent crystalline sheets in the different bulk layered materials.[7–11] The variety of such physical properties inspired the idea of using 2DM as building blocks to assemble vertically-stacked structures in which different layers are kept together by vdW interactions – the so-called van der Waals heterostructures (vdWH).[12,13] The resulting systems also possess a layered structure analogous to that of graphite and other layered systems, with the fundamental difference that the atomically-thin planes differ from one another, and the interlayer alignment is determined by the mechanical superposition of the different layers,[14] which is *a priori* difficult to control with an atomic precision. Based on these artificial systems, atomically-thin devices with unconventional functionalities have been demonstrated,[15] such as (tunnelling) transistors,[16] p-n and tunnelling diodes, [17,18] photovoltaic elements, light-emitting diodes/transistors.[17,19] From a fundamental point of

view, the properties of the 2DMs arranged in vdWHs are profoundly different from those of their isolated components, since interlayer vdW interactions, although weak in nature, affect dramatically their electronic,[20–23] optical,[17,24] and magnetic[25–27] properties. In this regard, making use of 2DMs stacked in vdWH represents a valuable strategy to fabricate novel artificial materials with ad-hoc properties.[12,13,15]

Molecules offer a unique opportunity to widen the horizon of vdWHs. Unlike inorganic 2DMs in which the properties of a single layer are determined by the pristine atomic arrangement,[9,10] the almost unlimited degrees of freedom in molecular design offer the possibility to synthesize molecules with functional groups with electronic, optical and magnetic properties that can activate specific atomic/molecular interactions with 2DMs.[28–30] While the number of potentially available 2DMs is estimated around several hundreds,[31] an almost unlimited number of molecules can be synthesized[32,33] (**Figure 1**). Following the original visual comparison between inorganic 2DMs and flat LEGO bricks,[12] molecules can be considered as dot-like quasi-0D LEGO blocks, which form continuous 2D layers onto inorganic 2DMs, with thicknesses ranging from that of a monolayer up to several tens of nanometers (Figure 1). While atoms within *inorganic* monolayers are covalently bound,[7–10] molecules within *organic* layers are held together by weaker non-covalent interactions such as vdW, dipole-dipole or electrostatic forces.[34–41] Importantly, supramolecular interactions can be mastered[42] to generate self-assembled *crystalline* organic films at the surface of inorganic 2DMs. Within such molecular layers, molecules can be positioned with atomic precision and be oriented along a given direction (Figure 1).[34–41] Thanks to the periodicity provided by the long-range crystalline ordering, analogous molecule-2DMs interactions recur at each "molecular site" at the organic/inorganic interface, inducing a surface modification which is spatially homogeneous at a mesoscopic scale. As a consequence, the local variations in the

energetics of 2DMs caused by the presence of individual molecules collectively sums-up yielding non-local macroscopic effects indeed arising when the 2DM surface is covered by a crystalline molecular assembly. The interactions of such molecular layer with the inert surface of 2DM are mediated by vdW forces analogous to those between different inorganic sheets, [34–40,43] so that similar interface effects can be envisaged in both cases, making organic/inorganic architectures the hybrid equivalent of fully-inorganic vdWHs. The analogy is even more profound if one considers that crystalline molecular monolayers can be obtained[44–69] that can be integrated in complex multi-layered heterostructures composed of alternating organic/inorganic single layers.

Likewise their inorganic counterpart, hybrid vdWHs have been characterized and employed with two distinct goals, i.e. demonstrating novel device architectures[70–77] and modifying fundamental physical properties of 2DMs[68,78–82]. In the first case, the electrical current flows *vertically* from a 2DM into a molecular thin film. Hence, the molecular layer is required to transport electrical current, and as such organic semiconductors are employed. In the second case, molecule-induced modifications in 2DMs are typically read out electrically in *lateral* devices, wherein the electrical current flows within the 2DM under the influence of the nearby molecular layer. In this case, the modulation in the physical properties of 2DMs is determined by their interaction with (insulating) molecules featuring specific functional groups, for instance electron acceptors or donors.

Here, we discuss recent progress in the field of hybrid organic/inorganic vdWH, by highlighting the most promising directions as well as the open challenges in the field. The results are presented in order of increasing complexity and control over the molecular/2DM systems. In section 2 we present the device perspective of hybrid vdWHs, analysing novel device architectures in which the molecular layer is not intended to introduce fundamental

variation in 2DMs, but rather to provide semiconducting functionalities to the hybrid heterostructure. From section 3, we change the point of view and focus on the molecule-induced modification in 2DM, describing the nanoscale effects which take place whenever molecules are in contact with the surface of 2DMs. In section 4, we explain how molecules with unique capabilities with no analogue in inorganic materials can be exploited to impart novel responsivity to 2DMs. Finally, in section 5 we focus on supramolecularly engineered hybrid vdWHs, by showing how the control over the structure of the organic layer allows to extend the nanoscale effects described in Section 3 over macroscopic distances, resulting in a very fine manipulation of the intrinsic electronic properties of 2DMs.

We highlight that in all these experiments the crystal structure of 2DMs is unaltered, and the molecule-induced modification are mostly induced by vdW or electrostatic forces. In this way, the outstanding electronic properties of 2DMs[7–11] are retained and coupled to molecular capabilities. In contrast, different strategies are appearing to modify the properties of 2DMs by covalent molecular decorations,[83–87] so that modification in the 2DMs arise from a direct rearrangement in their crystal structure. Such approach, which has the potential to relief crystalline defects,[85] is fundamentally different from that of the non-covalent hybrid vdWH discussed so far, and will not be discussed in this Progress Report.

2. van der Waals heterostructures: a device perspective

Electronics based on 2DMs and molecules is nowadays a widely explored research field. In several works, graphene is used as a conductive transparent electrode providing electrical contact to an organic semiconductor, both in lateral (transistor-like)[88–90] or in vertical geometries.[91] For a complete overview about electronics based on graphene/organic semiconductors, we refer the reader to a recent review.[92] In this section, we will focus on

two device architectures, which clearly show the potential of hybrid vdW heterostructures to fabricate unconventional devices with unique capabilities.

In both cases, the devices exploit the semiconducting nature of certain organic molecules, whereas a 2DM/molecules interface plays a central role in determining the device performances. In particular, both device architectures are characterized by the presence of a relatively thick and structurally uncontrolled organic thin film physisorbed onto different 2DMs, typically MoS_2 or graphene. As we shall demonstrate, the devices benefit from a controllable modification of the energetics at 2DM/molecules interfaces, achievable through the application of an electric field generated by a gate terminal.

2.1 Gate-tunable p-n heterojunctions: anti-ambipolar transistors

Due to its intrinsic n-type doping[5,93], MoS_2 can be employed in combination with another p-type material to demonstrate p-n heterojunctions. Such possibility was initially demonstrated for all-inorganic heterostructures, in which WSe_2 acted as p-type semiconductor.[17] The possibility to use an organic semiconductor as hole conductor was successively explored by different groups in 2015.[70–72] In all cases a device architecture similar to that shown in **Figure 2**a was employed, in which one metal electrode contacts a mechanically-exfoliated n-type MoS_2 flake, and the second one is solely connected to a p-type organic film. The partial overlap between the organic films and the MoS_2 flake defines a p-n junction while a Si/SiO_2 substrate was used to apply a back gate. As compared to fully inorganic vdWHs, the use of organics allows a facile device fabrication by avoiding the cumbersome flake-to-flake alignment and thus paving the way for up-scalability.

The device fabrication started by the definition of (at least) two Au electrodes in the proximity of a MoS_2 flake, one being in contact with it and the other being separated by a distance in the

few-micrometers range. Then, an organic layer was deposited contacting the separated Au electrode and the MoS_2 flake. In one case, the p-type organic semiconductor was a rubrene crystal[70], which was mechanically placed onto a pre-contacted MoS_2 flake by optical alignment under a microscope. In the other works[71,72], two step e-beam lithography was exploited to first define the Au electrodes and subsequently to open a window in a resist film to define the active device area by exposing only the region in which the organic semiconductor was required. A thin film of small molecule (copper phthalocyanine[71] and pentacene[72]) was then evaporated on the so-obtained structure, with the resist acting as a mask and ensuring electrical insulation between the semiconducting molecules and the Au electrodes on MoS_2.

The so-obtained 2DM/organic p-n junctions exhibited a rectifying (diode-like) behaviour which could be modulated by the back-gate potential. Here, we discuss in detail the electrical characteristics of the devices based on the MoS_2/pentacene heterojunction,[72] but similar results were obtained in the other cases. Figure 2b shows a 3D plot of the transfer curves measured at different applied gate potentials in MoS_2/pentacene devices. At either extremes of the gate range, the MoS_2/pentacene heterojunction is characterized by a nearly insulating state, while at intermediate values it displays a highly rectifying output. The rectification at intermediate gate voltages can be understood in analogy to any p-n junction, i.e. high current flows through the device when the drain-source polarity allows electrons to be injected into the n-type MoS_2 and holes into the p-type pentacene, while it is several orders of magnitude lower for the opposite polarity. Instead, the insulating behaviour at large gate bias can be understood on the basis of the electrical characterization of the separate layers of MoS_2 and pentacene, as addressed separately (Fig. 2c). Since MoS_2 (pentacene) is an n-type (p-type) semiconductor, it is OFF at large negative (positive) gate voltages, i.e. it behaves as an

insulator. Since the heterojunction is composed of the series of the two materials, the overall current reflects the rule of addition of resistances in series, and as such it is sizable only in the intermediate voltage region, in which both materials are ON. The term anti-ambipolarity was coined to describe such electrical characteristics, well-capturing the unconventional behavior of 2DM/organic heterojunctions.

The photoresponse of these systems was also characterized for the three systems highlighted in Fig. 2.[70–72] For the MoS_2/pentacene heterojunction displayed in Figure 2d, a photocurrent map was performed in which a diffraction-limited laser beam was scanned over the device, while the current was recorded as a function of position. Figure 2e shows the map of photocurrent, which surprisingly indicates that the photocurrent is mostly generated at the one-dimensional MoS_2 flake boundary. Indeed, one would naively expect the photocurrent to be generated at every position within the p-n junction, i.e. all over the region of overlap between MoS_2 and the organic layer, and not only at the edge of the 2DM. This finding was explained on the basis of the different direction of the local electric field and on the different morphology of the organic layer on the MoS_2 and outside of it, indicating that the MoS_2 edge possessed a primal role in the determination of the photoresponse. This characteristic represents a clear difference with respect to fully-inorganic vdWH,[17] and the presence of such sharp quasi-1D interfaces might lead to other unique features, such as light emission from a 1D region. Indeed, the possibility to obtain hybrid gate-tuneable light-emitting p-n junctions based on 2DM/molecules remains so far unexplored. More recently, the role of charge traps in similar structures was investigated in detail[94], and an optimization of the device characteristics was accomplished by adopting high quality organic single crystals instead of polycrystalline films[95].

2.2 Vertical field-effect transistors: graphene barristors

The 2D nature of graphene enabled the demonstration of a novel vertical field-effect transistor device architecture, called barristor.[96] The latter is based on the unique possibility of modulating the Shottky barrier at a graphene/semiconductor interface. After the first demonstration of a barristor based on a graphene/Si interface[96] and of analogous device structures based on fully inorganic vdW heterostructures[16,97–99], it was soon realized that organic semiconductor could well be used in the same device architecture[73], since an energy barrier for carrier injections also forms at the interfaces between conductive materials and organics.[100–102]

The typical device architecture of a graphene/organic barristor is portrayed in **Figure 3**a. Graphene is used as a source terminal in a vertical structure composed of an organic semiconductor layer contacted by a top metal contact (the drain), while a Si/SiO_2 substrate is employed as gate. The working mechanism is explained with the help of Fig. 3b-c, in which the organic semiconductor is assumed to have n-type character. In analogy to the case of common metals, a potential barrier for charge carriers (called Schottky barrier) is formed at the interface between graphene and semiconductor, ruling the charge injection from graphene into the organic semiconductor. Typically, in air environment the graphene is p-doped,[103] thus the energy barrier to n-type organics is significant, resulting in an unfavorable charge injection from graphene to the semiconductor. Therefore, in the absence of an applied gate voltage, graphene/organic/metal tri-layers behave as a so-called Schottky diode, with strongly asymmetric electrical characteristics showing low (high) current when electrons are injected by graphene (top metal contact). Unlike the case of common metals, the work function of graphene can be tuned by the application of an external gate potential,[104] which effectively

changes the barrier height.[96] In turn, this effect strongly affects the charge injection, which can be favoured by the application of a proper (negative) gate bias.

The electrical characteristics of a C_{60}-based barristor are displayed in Figure 3d, showing an almost ideal modulation of the electrical current injected from the graphene.[74] The graphene/C_{60}/top metal contact (Al in this case) is asymmetric at $V_{GS} = 0$ V, since a relatively high energy barrier prevents an efficient electron injection from graphene into C_{60}. The application of a gate voltage effectively tunes the Schottky barrier, resulting in a four-orders-of-magnitude modulation of the injected current from an OFF state (insulating) to an ON state (conductive). A careful study of similar C_{60}-based vertical transistors[75,77] revealed that the change in the injected current was not only due to a modulation of the energy barrier, but also to the fact that the graphene layer does not perfectly screen the gate electric field, which extends in the C_{60} layer causing a local redistribution of charge carriers. Analogous results were demonstrated in very similar C_{60}-based vertical transistors,[74–77] as well as in other n-[105–107] and p-type[73,77,105–109] organic semiconductors. Moreover, a complementary inverter was fabricated by connecting an n-type and a p-type vertical transistors. While the gain was not very high (as shown in Figure 3e), it could certainly be further optimized, thus opening the way to logic operations based on barristors.[105,106]

In light of these results, vertical field-effect transistors based on hybrid vdW heterostructures hold a great technological potential, since their fabrication is straightforward, up-scalable and applicable on flexible substrates, yielding graphene-based transistors featuring relatively high ON-OFF ratios, which cannot be obtained in normal graphene based field-effect transistors. Moreover, the relatively low mobility of organic semiconductors,[110] does not play a primal role in the determination of the barristor performances.

Finally, we highlight that so-far uncharted effects might be demonstrated in barristor

architectures analogous to those described here. For instance, we propose a device architecture in which light emission could be switched ON and OFF by a gate voltage. In such device, schematically shown in Fig. 3f, a light-emitting organic p-n bilayer sandwiched between two graphene sheets onto a Si/SiO_2 substrate, and the band alignment can be carefully controlled by graphene doping.[106] Under optimized conditions, light emission would only take place when a sizable current flows through the stack, i.e. when a proper gate voltage is applied, while no light emission is expected in the OFF state. In this regard, hybrid vdWH might enable the demonstration of unprecedented multifunctional light-emitting vertical transistors.

3. Molecules on 2D materials: doping and beyond.

The works presented in the previous section clearly indicate the technological relevance of hybrid vdWHs, the latter enabling the fabrication of unconventional devices with unique capabilities. From this section on, we focus on the intriguing possibility to modify intrinsic properties of 2DMs in a controlled manner via non-covalent interactions with molecules and assemblies thereof. In particular, in this section we describe the effects which take place at the nanoscale when molecules are in contact with 2DMs. In subsection 3.1, we will first focus on the nanoscale origin of the doping effect,[78,79,111,112] i.e. the change in charge carrier concentration within 2DMs. Later on (subsection 3.2), we will show how nanoscale effects at molecules/2DMs interfaces can be tailored at a more profound level, to deeply affect fundamental characteristics of 2DMs, such as their superconductivity and magnetic properties. Within this discussion, it will emerge that the molecules employed to modify the intrinsic properties of 2D materials possess characteristics which are markedly different from those of the organic semiconductors employed in the device architectures described in Section 2.

3.1 Nanoscale origin of molecular doping.

Already in the early days of graphene, it was demonstrated that the interaction of gas molecules with the graphene surface can induce a notable change in the charge transport properties of the latter[78,111], effectively introducing additional charge carriers, and thus acting as dopant species. This first report marked the birth of the so-called molecular (or chemical) doping of graphene, a field which grew steadily in the next years.[79,112–115] Similar effects were successively measured in mono- and few- layers of TMDCs[80,116–119] and X-enes[120]. Nowadays a rather vast literature exists about molecular dopants of 2D materials, and well-established concepts inherited by organic electronics have been applied to select or design p- or n- type molecular dopant.[121] In this section, we briefly review the main mechanisms which lead to the doping, not with the purpose of being comprehensive, but rather to give a nanoscale insight into the effects which take place at 2DM/molecules interfaces and which are capable of modifying the electronic properties of 2DMs.

Doping effects are typically explained in terms of charge transfer[112] or molecular-dipole-induced shift in work function.[115] In the case of charge transfer, the doping effects are caused by the energy level alignment, which makes it favourable for an electron to be transferred from the 2DM to the molecule (or viceversa). In contrast, dipole-mediated doping can potentially take place any time that polar molecules are physisorbed on 2DMs. In this case, the electric fields emanating from the dipoles act as a local gate, capable of shifting the 2DM work function and thus inducing doping.[122] More specifically, the extent of the doping also depends on the mutual orientation of the dipolar group with respect to the normal to the surface. While the two effects are normally concomitant and difficult to disentangle, **Figure 4** displays two exemplary cases in which either effect was dominant in the determination of the

doping in few-layer TMDC. Neutral benzyl-viologen was used to induce pure charge transfer and act as electron donor, as shown in Figure 4c.[123] Benzyl-viologen has one of the lowest reduction potentials among all electron-donor organic molecules, so that in neutral form it transfers electrons to electron acceptor materials, such as MoS_2[123] or graphene.[124] This can be understood on the basis of the energy diagram shown in Fig. 3b, which depicts the energy level between the conduction band edge of MoS_2 and the reduction potential of the BV molecule. Since there is an offset between the MoS_2 conduction band and the molecular reduction potential, it is energetically favourable for an electron to be transferred from the molecule to the MoS_2. This effect was read out electrically in transistors as an increase in the concentration of free electrons available for charge transport, i.e. n-type doping (Figure 4c). In contrast, in the case of Figure 4d-f, octadecyltrichlorosilane OTS was demonstrated to induce p-type doping on WSe_2.[117] OTS are wide bandgap molecules, with energy levels lying far in energy from those of WSe_2, thus hindering efficient charge transfer. Therefore, in order to explain the doping effects, the authors hypothesize that OTS molecules are self-assembling on the WSe_2 surface in such a way that aligned molecular dipoles induce a shift in the WSe_2 work function readable at the device level as a shift in threshold voltage, which is ascribable to a p-type doping (Fig. 4e-f). Therefore, the molecular self-assembly, which ensures that all molecular dipoles are oriented along the same direction, has a fundamental role in the determination of the effects taking place at molecules/2DMs interfaces, even if in this case the role of the molecular orientation was only a posteriori inferred on the basis of the electrical results, without a direct characterization of the nanoscale ordering, e.g. by means of Scanning Tunneling Microscopy (STM) or X-ray based methods. The importance of studying the nanoscale assembly as well as the opportunity offered by its precise control will be treated in detail in Section 5.

Due to the ubiquity and reproducibility of the reported doping effects, it is often assumed that when molecules are physisorbed on 2D materials *only* doping should be expected. Here we like to point out that while doping effect are indeed a key feature of 2DM/molecules interfaces, recent reports seem to indicate otherwise. Molecular doping effects represent only *one* among the possible effects taking place at the interface between organics and 2DMs.

3.2 2DMs/molecules interactions beyond doping: towards modification of fundamental properties.

In this section, we shall review two experiments in which molecular decoration is tailored to induce significant changes in fundamental properties of 2DMs. In a first experiment, molecular physisorption is exploited to open a bandgap in bilayer graphene; in a second one, to modify the superconducting transition in a 2D In layer. In both cases, control over the molecular assembly does not play an important role, while we shall discuss in the section 4 studies in which active control over molecular arrangement is fully exploited to modify the properties of 2DMs in a controlled manner.

In bilayer graphene, a bandgap can be opened and manipulated by out-of-plane electric fields that break the spatial inversion symmetry.[125,126] This task has been achieved by using devices in dual gate configuration,[127–133] or by means of molecular dopant species which exert significant electric fields to graphene.[124,126,134] A chemical-engineering approach to the bandgap opening in bilayer graphene was demonstrated by Park et al.[135]. In their study, the authors employed bilayer graphene mechanically exfoliated onto a SiO_2 substrate which was previously covalently functionalized with a self-assembled monolayer exposing an n-doping amino group (NH_3). Subsequently, a layer of (p-dopant) 2,3,5,6-tetrafl uoro-7,7,8,8-tetracyano- p –quinodimethane F_4-TCNQ[112] was evaporated onto the top graphene surface,

forming a sandwich structure in which the bilayer graphene was in contact with a bottom n-type and a top p-type dopant. In these conditions, strong electric fields perpendicular to the bilayer graphene developed, effectively opening a bandgap. These results were confirmed by a study of the electrical characteristics of the bilayer graphene. In particular, it was shown that not only the amino-SAM introduced a shift of the Dirac point towards negative values, indicative of n-doping, but also increased the I_{ON}-I_{OFF} ratio as compared to the case of bare SiO_2 (**Figure 5**a). This result was explained by the opening of a bandgap due to the electric fields introduced by the bottom layer (Figure 5b). The deposition of the top F4-TCNQ layer would induce p-type doping and further increase the I_{ON}-I_{OFF} ratio in bilayer graphene, demonstrating the widening of the bandgap as a consequence of an enhanced perpendicular electric fields across the sandwich structure (Fig. 5b). Joint electrical and optical characterization revealed a significant bandgap between 100 and 200 meV, therefore demonstrating that significant variation in the band structure of a 2DM could be achieved thanks to molecular decorations.

In a more recent study,[81] Yoshizawa et al. investigated the effect of a molecular adlayer on superconductivity in 2DMs. In particular, the authors studied heterostructures composed of two phthalocyanines coordinating different metal ions (Mn, Cu) onto an In monolayer epitaxially grown onto Si (Figure 5c). It was demonstrated that the critical temperature to enter the superconducting regime in heterostructures could be controllably modified, and in particular it could be increased or decreased by the interaction with an adlayer of Cu- or Mn-phthalocyanine, respectively (Figure 5d). To unveil the mechanism behind the measured effects, the authors combined a variety of techniques, including scanning tunneling microscopy (STM), angle-resolved photoemission spectroscopy (ARPES), X-ray magnetic circular dichroism (XRMCD) and *ab initio* calculations. In the Mn-case, a d- molecular

orbital bearing a magnetic momentum extend to the In monolayer, suppressing the superconductivity due to the magnetic pair breaking effect, therefore decreasing the transition temperature. The same effect was not found when Cu was employed, in which case d-orbitals are confined within the molecule. The increase in transition temperature was then explained by a molecule-induced p-type doping of the In layer. The results of these study show the possibility to tune fundamental parameters of 2DMs, and highlight the importance of a comprehensive understanding of the effects occurring at the 2DM/molecules interface. In some cases, not only charge- but also spin-related phenomena should be taken into account to draw a full picture of hybrid vdWHs.

The effect of molecular decoration on a superconductive 2DM was also investigated in another recent work.[136] In this case, the decoration of superconductive $NbSe_2$ with hydrazine molecules was shown to modify the magnetism of the 2DM, leading the authors to the conclusion that a ferromagnetic state was induced in $NbSe_2$. Such effect was explained on the basis of a structural modification in the $NbSe_2$ structure, triggered by the hydrazine molecules. However, the system studied were rather different from the perfect 2DMs considered so far – the $NbSe_2$ was chemically obtained by Li intercalation, resulting in defective nanosheets casted over a substrate or assembled to form a relatively thick film. The exact role of the hydrazine molecules was only indirectly inferred and supported by calculation, but direct nanoscale evidence of the proposed mechanism was not provided. Further studies should be performed to confirm that hydrazine-induced ferromagnetism is maintained in ideal $NbSe_2$ at the monolayer level.

The modulation of intrinsic magnetic properties of 2DMs by proximity of molecular adlayers with peculiar spin textures is an extremely intriguing direction in the 2DM research which is still in its infancy. While long-range magnetic order was found in a molecular assembly on

graphene,[55] whether or not (ferro)magnetism can be induced in a 2DM by proximity effect to a molecular assembly is still an open question.

4. Hybrid van der Waals heterostructures with additional molecular functions.

In the previous section, we have described how the interaction between ad-hoc functional groups and 2DMs results in a modulation of the properties of the latter. Here, we take a step further by describing the effect on 2DMs of specific functional groups which have no analogous in inorganic systems. Certain moieties possess optical,[137–139] magnetic[140–142] and electronic[143,144] properties that can be controllably switched between two (meta-) stable states in response to external stimuli. Such molecular switches can be combined to 2DMs to demonstrate novel devices with a stimuli-responsive nature inherited by the molecular layer. Importantly, thanks to their ultra-high surface sensitivity, the electrical characteristics of 2DMs can be modified by a switch taking place in a physisorbed adlayer, without need of strong chemical bonds which would introduce structural and electronic defects in the structure of 2DMs. Therefore, the impressive electrical characteristics of pristine 2DMs can be retained and coupled to the unique functions of molecular switches to demonstrate high-performance multi-responsive opto-electronic or magneto-electronic devices. In particular, we shall describe experiments in which spin-crossover and photochromic molecules are employed to introduce a variation in the electrical characteristics of 2DMs.

4.1 Spin crossover molecules.

The spin crossover phenomenon involves the controllable switching process between two molecular states characterized by different spin configurations, namely a high spin, HS and a low spin, LS configuration.[141,142] Such effect takes place in metal-organic complexes in

which typically a Fe atom is coordinated by organic ligands, and can be triggered by different external stimuli, such as temperature, pressure, electrical potential and light. The possibility to read out the spin state of spin-crossover molecules on the surface of 2DMs by transport measurements was demonstrated only recently.[145] In this study, a continuous film composed of spin-crossover molecules assembled in nanoparticles[146] was deposited on the surface of CVD graphene (**Figure 6**a). From previous studies, it was known that temperature could be used to switch such SCO nanoparticles from a LS state below approximately 320 K to a HS state above approximately 380 K. Between these two temperatures, the SCO nanoparticle displayed a bistable hysteretic behaviour.

The resistance of CVD graphene was measured as a function of temperature and gate voltage in a four-probe contact configuration before and after decoration of the device with a layer of spin-crossover nanoparticles. It was found that the presence of the SCO nanoparticles induced p-type doping, recorded as a positive shift in the position of the charge neutrality point. The measurement of the electrical characteristics of the graphene/SCO system are shown in Figure 6b as a function of temperature for the heating (top) and cooling (bottom) modes. While in the former case a pronounced decrease of the resistance was observed above the switching temperatures of 374 K, in the latter case a specular resistance increase was observed below 327 K. The resistance switch is even more evident in Figure 6c, in which the resistance at the Dirac point is plotted as a function of temperature. Such variation in the graphene resistance, which was not measured for the pristine CVD graphene, resembled and closely matched the switch and hysteresis of the SCO complex, demonstrating that the spin transition could give rise to a change in the charge transport characteristics in graphene which can be detected at the device level. According to the authors, such electrical readout of the magnetic state was mediated by a change in the dielectric constant of the SCO film, which accompanies the spin

transition and modifies the remote interfacial phonon scattering, responsible for the degradation of graphene mobility.

This investigation clearly shows that the magnetic switch of SCO nanoparticles can be detected in the electrical transport of graphene devices. As compared to other molecular switches (see below), the effects presented in this study are relatively weak. Stronger changes in the graphene characteristics would be expected if the metal ion group in the SCO were placed closer to the 2DM surface. In this regard, the synthesis of on-purpose SCO, designed to self-assemble on the 2DM with the central ion in close proximity to the surface would be highly beneficial to amplify the measured effects. An interesting development could be the investigation of the effect of the SCO switch onto the graphene spin-related properties (e.g. spin lifetime).

4.2 Photochromic molecules.

Photochromic molecules can be reversibly switched upon irradiation at selected wavelengths between two isomers characterized by very different properties.[147] The most widely used photochromic molecules are azobenzenes,[137] diarylethenes[138] and spiropyrans.[139] In each case, the isomerization introduces a major change in different molecular properties. In particular, a significant variation in molecular spatial arrangement exists between the so-called *trans* and *cis* configuration, that feature different conductivity, in azobenzenes.[137] As for diarylethenes, a large energetic change in the electronic levels accompanies the transition between the open and the closed form[138] whilst a sizeable molecular dipole intensity does occur for spiropyrans.[139]

As compared to the case of SCOs, the study of hybrid vdWH comprising a layer of photochromic molecules is in a more advanced stage. A pioneering study focused on

graphene as standard 2DM, showing a light-induced response in its electronic characteristics when covered with azobenzenes.[148] In this case, a graphene field-effect device was covered with a physisorbed layer of photochromic molecules (Figure 6d). The presence of the azobenzenes (in *trans* form) was found to shift the Dirac point towards positive values as compared to the pristine case, introducing significant p-type doping (Figure 6e). The device was then irradiated by UV light to induce the *trans*-to-*cis* switch in the azobenzene layer. As a consequence of the UV irradiation, a small shift of the Dirac point to lower values was observed, corresponding to a reduction in the p-type doping. The full p-type doping of the *trans* form could be recovered by irradiation with visible light, showing the reversibility of the effect (Figure 6e). The same effect could be followed by Raman microscopy[149,150] by monitoring the position of the G-peak, as shown in Figure 6f. Initially, the G peak lies at 1581 cm^{-1}, indicative of relatively low intrinsic doping.[151] After the deposition of the azobenzene derivative in the *trans* form, the G peak shifted to 1591 cm^{-1}, indicative of significant doping. UV light irradiation was found to decrease the doping level, shifting back the G peak to 1588 cm^{-1}. Later, a similar reversible (n-type) doping was demonstrated employing spiropyrans as photochromic molecule.[152] In other experiments, graphene was used as an electrode to monitor the change in the current within a layer of photochromic molecules.[153,154] For a full overview of the effect taking place when carbon-based materials are decorated by photochromic molecules, we refer the reader to a recent review.[155] MoS_2 was also employed in vertical configuration as a semiconducting material for demonstrating light-switchable vertical diodes.[156,157] Moreover, it has been recently shown that the photoluminescence of MoS_2 on a photochromic monolayer depends on the isomerization of the latter.[156] However, to the best of our knowledge, no reports have appeared showing light-tunable characteristics

in field-effect devices based on transition metal dichalcogenides/photochromics heterostructures.

While these experiments show the intriguing possibility to modulate the electrical characteristics of 2DMs with a physisorbed layer of photochromic molecules, in several cases it was not possible to fully explain the mechanisms leading to the measured effects due to a lack of control over the nanoscale molecular ordering. A higher control over photochromics/2DMs heterostructures will be key to understand and optimize their unique photo-responsivity to demonstrate novel devices combining the capabilities derived by the molecular layer with the high electronic performances of 2DMs. Finally, we point out that other photochromics could be employed in the future in analogous studies to optimize and engineer the doping effects. For instance, the modification in the electronic levels of diarylethenes might be effective to achieve tuneable charge transfer to 2DM.

5. Molecular assembly in hybrid van der Waals heterostructures: functional materials at will

While in Section 3 and 4 we have discussed how functional groups introduce modifications in the electrical characteristics of 2DMs, here we show that a precise control over the molecular ordering can lead to further effects which can be manipulated with a high level of control and predictability.

Isolated molecules induce strong modifications in the energetics of 2DMs, which are confined within a small quasi-0D region localized around the molecule.[158] This effect is markedly different from the homogeneous 2D modifications obtained by interfacing different inorganic 2D materials.[12,13] In this context, supramolecular chemistry holds a huge potential since it allows to arrange molecular groups bearing on-demand functions at desired spatial locations

onto the surface of 2DMs with an atomic precision.[34–40] Spontaneous yet controllable self-assembly can be tuned in order to create highly-ordered molecular lattices on the surface of 2DMs, in which molecule/substrate interactions repeat themselves periodically at each molecular site. In this regard, the supramolecular assembly might be considered as a bridge connecting the quasi-zero-dimensionality of molecules to the two-dimensionality of inorganic single layers.

Several groups have studied the process of molecular self-assembly on graphene in the real space by Scanning Tunneling Microscopy.[44–67] These studies often focused epitaxial graphene grown onto metallic[47–49,52,54–56,66,67] or semiconducting SiC surfaces[44–46,50,51,53,57,58,61,64], and recently also on graphene transferred onto insulating SiO_2 or Boron Nitride.[59,60,62,65,158–163]

Very often, the molecular arrangement on graphene and on highly oriented pyrolytic graphite (HOPG) is analogous.[63] Indeed, the process of molecular self-assembly at surfaces is driven by molecule-molecule and molecule-substrate vdW interactions, which are akin for graphene and HOPG, and also for most layered materials, including transition metal dichalcogenides.[163–165] Therefore, well-established concepts inherited by the three-decade-long research in supramolecular chemistry at the surfaces[43] can be exploited to controllably arrange functional groups on the basal plane of 2DMs.

While in several cases the molecular assembly and its properties represent the main focus of STM studies,[44–67] only a few reports address the effects of a given molecular assembly on the electronic properties of 2DMs.[68,159–163] In these cases, an STM study of the molecular assembly on a 2DM (typically graphene) is combined to the investigation of the electrical properties of the same system, addressed at the macroscopic level (for instance, in devices). While in some cases the ordered assembly is investigated as a further characterization

complementary to the device study, [159–161,163] in other works it plays a central role. [68,166,167] Inspired by the latter works, we will highlight a few results that indicate how the possibility to tame the molecular assembly on 2DMs can be exploited to create hybrid vdW heterostructures with on-design intrinsic properties. We also highlight here that molecular self-assembly takes place on the surface of BN, so that ordered organic semiconductors can be epitaxially grown onto an insulating substrates with atomic precision.[108,168] Based on such self-assembled semiconductors, organic field-effect transistors with optimized performances could be fabricated.[108,168] While this approach is certainly very powerful, it is beyond the scope of this Progress Report. Hence, no further highlight on such matter will be given, and we will rather focus on the modification induced on the 2DMs.

5.1 Alkane epitaxy on graphene

In a recent study, Yu *et al.*[166] demonstrated that the electrical properties of graphene on SiO_2 are improved becoming almost-ideal after the self-assembly on its surface of an epitaxial multilayer of the long alkane n-hexatriacontane (HTC, $C_{36}H_{74}$). The molecule was deposited on graphene by drop-casting, and the solvent was slowly evaporated (**Figure 7**a). In these conditions, alkanes were found to self-assemble forming crystalline layers with a thickness of approximately 100 nm. An accurate structural investigation of the molecular layer was performed by characterizing the growth of the organic layer at different stages making use of different techniques. The nanoscale arrangement of the first monolayer on graphene on SiO_2 was studied by STM, as displayed in Figure 7b. HTC molecules were found to adsorb flat on the graphene surface, by organizing in a closely packed lamellar structure, as commonly observed for long alkyl chains on graphitic surfaces.[35] The SiO_2-induced roughness of graphene did not to impede the formation of a well-ordered self-assemblies, which were

found to follow graphene morphology. Further, it was shown that the first HTC monolayers grew epitaxially on graphene, as demonstrated by the fact that the linear alkane chains are aligned along the graphene lattice (shown in Figure 7b, inset). Other characterization techniques, such as Selected Area Electron Diffraction (SAED), were employed in order to demonstrate that HTC molecules order perpendicularly to the basal plane of the graphene surface in the topmost part layer (as schematically shown in Figure 7a).

The electrical characteristics of graphene devices were measured before and after the formation of the HTC film, as portrayed in Figure 7c. The initial characteristics displayed an undesired p-type doping, which is commonly observed for graphene measured in ambient atmosphere, and is ascribed to the presence of water molecules and oxygen adsorbed on the graphene surface.[103] The formation of the HTC film introduces two main effects which were recorded in different samples: (i) the charge neutrality point was shifted towards the 0 gate voltage – indicative of a significant reduction of the undesired pristine doping; (ii) the graphene mobility was increased over three times in the different devices, in the overall making the electrical characteristics of graphene similar to those of suspended or BN-supported graphene.

These results were found to stem from the strong interaction between graphene and the HTC layer. In particular, the reduction of the undesired initial doping can be explained by considering that a replacement of water and oxygen adsorbates takes place with inert apolar alkane monolayers. The stronger vdW forces of the latter thus act as an effective passivation layer that screens the interaction of the 2DM with water and oxygen molecules. More specifically, the alkanes push out the undesired contamination (polar) molecules through a self-cleaning mechanism similar to that reported for vdWHs based on fully inorganic 2DMs.[98,169]

Instead, the increase in mobility was explained by a more subtle argument, fully supported by Density Functional Theory calculations. The interaction of graphene with the adsorbed HTC layer (considered as a whole) is stronger than that with the SiO_2 supporting layer. This interaction has the double effect of flattening the nanoscale graphene roughness, and lifting-up the graphene from the SiO_2 substrate, as evidenced by the DFT calculations summarized in Figure 7d. This theoretical finding is supported by a Raman characterization showing an increased tensile strain upon adsorption of the self-assembled HTC layer, in agreement with a previous report showing that an alkane layer could cause an elastic deformation of graphene. This strong HTC/graphene interaction has a positive effect on the two main mechanisms which are considered being the dominant sources of mobility degradation in graphene: structural corrugations and interaction with charged impurities. The former effect is partially relaxed thanks to the HTC-induced flattening, while the latter is a consequence of the graphene lifting, which results in a decreased coupling between graphene and the charged impurities in the SiO_2 substrate.

This investigation shows that HTC/graphene interactions can be exploited to optimize the electrical characteristics of graphene devices, representing a valuable strategy to emulate the effect of boron nitride substrates while at the same time offering a processability and up-scalability not (yet) achievable with BN. In perspective, full encapsulation of graphene between top and bottom alkane layers might confer it electrical characteristics rivalling those of suspended or BN-encapsulated graphene on boron nitride. We highlight that these results were achieved by employing a molecule without specific functional groups, which by itself, i.e. at the single molecule level, does not add any introduce any local modification in graphene. It is rather the collective effect of an Avogadro number of molecules self-assembled forming an ordered layer which generates the measured effect. In this regard, this

work represents a nice demonstration that molecules, when organized in ordered assemblies, can introduce modifications in the characteristics of the 2DMs which are intrinsically 2D and non-local.

5.2 Precisely controllable doping in hybrid vdW heterostructures

One exemplary case in which the control over the nanoscale molecular assembly allows a precise tuning of the properties of a hybrid vdWH is provided by the work of Phillipson *et al.*[166] In their study, the authors investigate the electrical properties of graphene covered by two different molecules, octadecylamine (ODA) and nonacosylamine (NCA). The two molecules are composed of a NH_2 amino head group bound to alkyl chains of different length, respectively 18 C atoms for ODA and 29 for NCA. In analogy with the study presented in the previous section, the alkyl chains are inserted in the molecule to induce a predictable self-assembly. Instead, amino groups are known to induce n-type doping on graphene,[111] therefore adding a distinctive function to the molecule. The idea at the basis of this study is summarized in **Figure 8**a. The alkyl chains drive a lamellar assembly in which they act as spacer between the NH_2 dopant groups. Hence, the use of molecules composed of alkyl chains with different length and terminating in the same dopant groups enables a precise control over the density of dopant species on the graphene surface. In turn, such precise control over the dopant density reflects into a tuneable doping effect, elegantly connecting the nanoscale molecular arrangement to macroscopic effects measured at the device level.

The nanoscale assembly of ODA and NCA was studied by STM and atomic force microscopy, as displayed in Figure 8b. Following the spin-coating of ODA and NCA from solution, analogous lamellar assemblies were monitored, in which rows of adjacent NH_2 doping groups

are separated by the different alkyl chain. Noteworthy, the different length of the alkyl chains of ODA and NCA results in a different separation between the doping groups, ultimately leading to a tuneable density of NH_2 dopants on graphene surface. Based on the STM measurements, the amine group density was 1.6 times higher for ODA compared to NCA, in agreement with the ratio of the alkyl chain lengths. Significantly, it was demonstrated that the same lamellar assembly was encountered on HOPG, on CVD graphene and even on the surface of a contacted graphene sheet, despite the presence of lithography residuals and of metallic electrodes.

The doping effect induced by the ODA and NCA on graphene was characterized optically by Raman spectroscopy and electrically by the fabrication and characterization of devices. In excellent agreement with the nanoscale characterization, a higher degree of doping was introduced by the ODA assembly, in which the dopant density at the surface is higher (Figure 8c). Moreover, the doping introduced in both cases was found to quantitatively scale as the density of dopant groups, so that the doping introduced by ODA was 1.6 times larger than that of NCA. Interestingly, we note that even in this case the mobility of graphene was improved after the deposition of the molecular layer, in agreement with the results of the previous study. The precision and predictability of the doping effects demonstrated in this work rival those of conventional inorganic semiconductors. Moreover, a similar assembly was encountered for very similar molecules on the surface of exfoliated MoS_2.[163] Therefore, analogous concepts for controlling the doping can be conveyed to the case of actual 2D semiconductor, in which a precise control of doping is vital for enabling electronic applications. In perspective, the possibility to exploit this approach to demonstrate doping over a spatially confined region on the flakes will be necessary to define lateral heterojunctions separating regions characterized by different doping within the same 2DM (such as p-n junction).

5.3 Periodic potentials in hybrid van der Waals heterostructures

Molecular self-assembly can be exploited to create a periodic potential on the surface of a 2DM. By using this approach, one could be capable of modifying profoundly the band structure of 2DMs. A strong modification of the graphene band structure by surface periodic potentials was studied theoretically,[170,171] and then experimentally demonstrated for the exemplary case of graphene on Boron Nitride. In this case, the relative alignment of the crystalline directions of the two flakes is extremely important, since it determines the periodicity of the potential, and thus its effect on the band structure of graphene.

We have recently showed that a tuneable 1D periodic modulation of the graphene surface energy takes place in hybrid vdWH in which an ordered molecular monolayer is deposited onto graphene. We have designed a molecule composed of a head bearing a light-reactive diazirine moiety and a linear tail, consisting of a long alkane. The chemical structure of the photoreactive headgroup was modified before deposition on graphene by simple irradiation in different solvents, which resulted in the incorporation of different atoms and yielded new molecules.

The resulting hybrid vdWH composed of the supramolecular layers of reacted and unreacted molecules on graphene was characterized structurally by STM at the nanoscale (**Figure 9**a and b), and electronically in mesoscopic devices. An analogous nanoscale assembly was imaged for the initial unreacted diazirine derivative and for the compound obtained by UV-irradiation in chloroform (Figure 9a and b), displaying the same unit cell parameters on HOPG and on CVD graphene on SiO_2. Instead, different doping effects were introduced in the electrical characteristics of graphene devices by assemblies of the unreacted and UV irradiated molecules, demonstrating different interaction between graphene and the molecular

heads in the two cases. On the basis of the structural and electronic characterizations, computational modelling was carried out to unravel the details of the molecular assemblies. The results of the device characterization could be fully explained on the basis of the orientation of different molecular dipoles in the head-groups on the graphene surface for the unreacted and UV irradiated molecules. The spatial modulation of the potential introduced by the orderly-oriented dipoles was calculated on the basis of the simulated assembly, and it is displayed in Figure 9 c,d. For both unreacted and UV-irradiated molecules, a 1D periodic modulation of the graphene surface energy was calculated, with the same periodicity (determined by the periodicity of the assembly) but different amplitudes (determined by the graphene/head groups interaction). Therefore, the intrinsic 3-fold symmetry of graphene could be broken by a controllable intrinsically-1D molecular decoration.

A 1D periodic potential similar to that shown in Figure 9c,d with periodicity in the few-nm-range and amplitude of a few-hundred millivolts was predicted to effectively induce an anisotropic propagation of charge carriers in graphene along the different directions of the potential.[170,171] A demonstration of anisotropic transport in graphene subjected to such molecular 1D periodic potential has not yet been provided, since the electrical measurements were performed over micrometric devices covered by several crystalline domains with different lamellar orientation. In perspective, the challenge for organic and supramolecular chemists will be the design of molecules capable of forming single domains over micro-metric distances addressable at the device level.

Conventional top-down approaches fail to reach the same resolution and accuracy, even when pushed to their extreme.[172] Indeed, the supramolecular assembly is self-aligned onto the graphene lattice, since its growth is templated by the crystalline directions of high symmetry in the substrate. Such self-alignment markedly differs from that of fully-inorganic vdWH, in

which the alignment between different 2DMs micrometric flakes is usually controlled by optical means during the mechanical superimposition of the different materials.[14] Moreover, we highlight that the amplitude and periodicity of induced potential can be anticipated and thus programmed by molecular design. In the same way, not only 1D, but any geometries can be achieved through the choice of proper molecular units forming the assembly.

Finally, the possibility to control molecular self-assembly to position individual dopant groups at desired spatial locations can be extended to the case of transition metal dichalcogenides (such as WSe_2 and MoS_2), since the molecular arrangement at the surface of all van der Waals substrates is analogous.[108,163,164,168] In semiconducting materials, Coulomb interactions are capable of modifying the energy levels locally generating p-n heterojunctions within single layer with interfaces as sharp as a few unit cells, as recently calculated for the case of single layer MoS_2.[173] Therefore, we propose the study of a system similar to that shown in **Figure 10**, in which a p-type molecular dopant (such as F_4TCNQ) co-assembles with inert alkyl chains onto MoS_2, to give rise to a lamellar assembly in which parallel rows of dopant groups are separated by the inert chains. In this case, one could precisely define alternating hole- or electron- rich regions, which might act as a series of consecutive p–n junctions at the molecular scale, in which the intrinsic n-type character of MoS_2 is locally modified by the local molecular doping. We are not aware of theoretical studies addressing the electronic or optical properties of such structures, but one might expect a modulation of the energetics of the MoS_2 band structure analogous to that shown in Figure 10c, with multiple potential wells which might give rise to anisotropy in the electrical conduction and affect profoundly the optical properties of the 2DM. We highlight that a similar modulation of the band structure of semiconductors is obtained at another dimensionality in 3D

heterostructures composed of different epitaxial layers, providing evidence for the interest in analogous structure for fundamental physics and technological applications.

6. Conclusions

In this Progress Report, we have discussed recent works in which 2DMs are combined to organic molecules, highlighting possible exciting developments of the field. We have pointed out that while individual molecules introduce local variation in the energetics of 2DMs, a large number of molecules collectively interacting with 2DMs introduces macroscopic modulation in the 2DMs properties. The molecular ensemble can be regarded as a continuous and homogeneous layer which interacts with 2DMs through vdW forces similar to those keeping together different 2DMs in vdWHs. In this framework, molecule/2DMs systems can be considered the hybrid equivalent of vdWHs, and in analogy to the fully inorganic version they can be used either for the demonstration of novel device architectures or for the creation of functional materials with properties on demand. The analogy between fully inorganic and hybrid vdWHs is even more profound, since molecules self-assemble forming ordered, crystalline 2D monolayers on the surface of 2DMs, which can be integrated in vertical stacks of materials. Moreover, thanks to the decades-long advances in supramolecular chemistry, the molecular assembly can be predicted and programmed at the synthesis stage, leading to self-assemblies which spontaneously align to the crystal structure of 2DMs with atomic precision. While these systems are starting to be explored, the field is open for new ideas and discoveries, as we have highlighted by discussing several possible future developments for the field. From a technological perspective, hybrid vdWHs might enable the demonstration of unprecedented multifunctional light-emitting gate-tunable devices. From a more fundamental point of view, the supramolecular control over the nanoscale assembly could be readily

extended to other semiconducting 2D materials and to other molecules, in which not only dopant groups, but other on-demand capabilities can be positioned with atomic position. For instance, one could control and optimize the positioning of magnetically active molecules with uncompensated spins over 2DMs, and alter the magnetic properties of the resulting material. Moreover, precise control over the nanoscale assembly of molecular switches might allow to better understand the mechanisms leading to macroscopic effects, and hence optimize the conductance switch in high performance devices. Finally, an experimental proof of the effect of supramolecular periodic potentials on the fundamental properties of 2DMs might open new horizons for the creation of functional materials at will. All the examples we have discussed above deal with bilayer systems, in which an organic (mono)layer covers the 2DM surface. However, by exploiting the same strategies, more sophisticated multi-layered structures could be conceived and realized, thereby building the foundations of a new class of hybrid materials for unconventional opto-spin-electronics.

Acknowledgements

We acknowledge funding from the European Commission through the Graphene Flagship (GA-696656), the FET project UPGRADE (GA-309056), the M-ERA.NET project MODIGLIANI, and the Marie Sklodowska-Curie IEF project SUPER2D (GA-748971), the Agence Nationale de la Recherche through the Labex projects CSC (ANR-10-LABX-0026 CSC) and NIE (ANR-11-LABX-0058 NIE) within the Investissement d'Avenir program (ANR-10-120 IDEX-0002-02), and the International Center for Frontier Research in Chemistry (icFRC).

Received: ((will be filled in by the editorial staff))

Revised: ((will be filled in by the editorial staff))

Published online: ((will be filled in by the editorial staff))

References

[1] K. S. Novoselov, A. K. Geim, S. V Morozov, D. Jiang, Y. Zhang, S. V Dubonos, I. V Grigorieva, A. A. Firsov, *Science* **2004**, *306*, 666.

[2] C. R. Dean, A. F. Young, I. Meric, C. Lee, L. Wang, S. Sorgenfrei, K. Watanabe, T. Taniguchi, P. Kim, K. L. Shepard, J. Hone, *Nat. Nanotechnol.* **2010**, *5*, 722.

[3] K. F. Mak, C. Lee, J. Hone, J. Shan, T. F. Heinz, *Phys. Rev. Lett.* **2010**, *105*, 136805.

[4] A. Splendiani, L. Sun, Y. Zhang, T. Li, J. Kim, C. Y. Chim, G. Galli, F. Wang, *Nano Lett.* **2010**, *10*, 1271.

[5] B. Radisavljevic, A. Radenovic, J. Brivio, V. Giacometti, A. Kis, *Nat. Nanotechnol.* **2011**, *6*, 147.

[6] L. Li, Y. Yu, G. J. Ye, Q. Ge, X. Ou, H. Wu, D. Feng, X. H. Chen, Y. Zhang, *Nat. Nanotechnol.* **2014**, *9*, 372.

[7] G. Fiori, F. Bonaccorso, G. Iannaccone, T. Palacios, D. Neumaier, A. Seabaugh, S. K. Banerjee, L. Colombo, *Nat. Nanotechnol.* **2014**, *9*, 768.

[8] F. Xia, H. Wang, D. Xiao, M. Dubey, A. Ramasubramaniam, *Nat. Photonics* **2014**, *8*, 899.

[9] M. Chhowalla, H. S. Shin, G. Eda, L.-J. Li, K. P. Loh, H. Zhang, *Nat. Chem.* **2013**, *5*, 263.

[10] D. Akinwande, N. Petrone, J. Hone, *Nat. Commun.* **2014**, *5*, 5678.

[11] B. Huang, G. Clark, E. Navarro-Moratalla, D. R. Klein, R. Cheng, K. L. Seyler, D.

Zhong, E. Schmidgall, M. A. McGuire, D. H. Cobden, W. Yao, D. Xiao, P. Jarillo-Herrero, X. Xu, *Nature* **2017**, *546*, 270.

[12] A. K. Geim, I. V Grigorieva, *Nature* **2013**, *499*, 419.

[13] K. S. Novoselov, A. Mishchenko, A. Carvalho, A. H. Castro Neto, *Science* **2016**, *353*, 461.

[14] A. Castellanos-Gomez, M. Buscema, R. Molenaar, V. Singh, L. Janssen, H. S. J. van der Zant, G. A. Steele, *2D Mater.* **2014**, *1*, 11002.

[15] Y. Liu, N. O. Weiss, X. Duan, H.-C. Cheng, Y. Huang, X. Duan, *Nat. Rev. Mater.* **2016**, *1*, 16042.

[16] L. Britnell, R. V Gorbachev, R. Jalil, B. D. Belle, F. Schedin, A. Mishchenko, T. Georgiou, M. I. Katsnelson, L. Eaves, S. V Morozov, N. M. R. Peres, J. Leist, A. K. Geim, K. S. Novoselov, L. A. Ponomarenko, *Science* **2012**, *335*, 947.

[17] C.-H. Lee, G.-H. Lee, A. M. van der Zande, W. Chen, Y. Li, M. Han, X. Cui, G. Arefe, C. Nuckolls, T. F. Heinz, J. Guo, J. Hone, P. Kim, *Nat. Nanotechnol.* **2014**, *9*, 676.

[18] L. Britnell, R. V Gorbachev, A. K. Geim, L. A. Ponomarenko, A. Mishchenko, M. T. Greenaway, T. M. Fromhold, K. S. Novoselov, L. Eaves, *Nat. Commun.* **2013**, *4*, 1794.

[19] F. Withers, O. Del Pozo-Zamudio, A. Mishchenko, A. P. Rooney, A. Gholinia, K. Watanabe, T. Taniguchi, S. J. Haigh, a K. Geim, a I. Tartakovskii, K. S. Novoselov, *Nat. Mater.* **2015**, *14*, 301.

[20] C. R. Dean, L. Wang, P. Maher, C. Forsythe, F. Ghahari, Y. Gao, J. Katoch, M. Ishigami, P. Moon, M. Koshino, T. Taniguchi, K. Watanabe, K. L. Shepard, J. Hone, P. Kim, *Nature* **2013**, *497*, 598.

[21] L. A. Ponomarenko, R. V Gorbachev, G. L. Yu, D. C. Elias, R. Jalil, A. A. Patel, A. Mishchenko, A. S. Mayorov, C. R. Woods, J. R. Wallbank, M. Mucha-Kruczynski, B.

A. Piot, M. Potemski, I. V Grigorieva, K. S. Novoselov, F. Guinea, V. I. Fal'ko, A. K. Geim, *Nature* **2013**, *497*, 594.

[22] R. V. Gorbachev, J. C. W. Song, G. L. Yu, A. V. Kretinin, F. Withers, Y. Cao, A. Mishchenko, I. V. Grigorieva, K. S. Novoselov, L. S. Levitov, A. K. Geim, *Science* **2014**, *346*, 448.

[23] B. Hunt, J. D. Sanchez-Yamagishi, A. F. Young, M. Yankowitz, B. J. LeRoy, K. Watanabe, T. Taniguchi, P. Moon, M. Koshino, P. Jarillo-Herrero, R. C. Ashoori, *Science* **2013**, *340*, 1427.

[24] M. M. Furchi, A. Pospischil, F. Libisch, J. Burgdo, T. Mueller, *Nano Lett.* **2014**, *14*, 4785.

[25] A. Avsar, J. Y. Tan, T. Taychatanapat, J. Balakrishnan, G. K. W. Koon, Y. Yeo, J. Lahiri, A. Carvalho, A. S. Rodin, E. C. T. O'Farrell, G. Eda, A. H. Castro Neto, B. Özyilmaz, *Nat. Commun.* **2014**, *5*, 4875.

[26] Z. Wang, D. K. Ki, H. Chen, H. Berger, A. H. Macdonald, A. F. Morpurgo, *Nat. Commun.* **2015**, *6*, 8339.

[27] W. Yan, O. Txoperena, R. Llopis, H. Dery, L. E. Hueso, F. Casanova, *Nat. Commun.* **2016**, *7*, 13372.

[28] W. Wu, Y. Liu, D. Zhu, *Chem. Soc. Rev.* **2010**, *39*, 1489.

[29] P. M. Beaujuge, J. M. J. Fréchet, *J. Am. Chem. Soc.* **2011**, *133*, 20009.

[30] S. Chen, Y. Liu, W. Qiu, X. Sun, Y. Ma, D. Zhu, *Chem. Mater.* **2005**, *17*, 2208.

[31] M. Ashton, J. Paul, S. B. Sinnott, R. G. Hennig, *Phys. Rev. Lett.* **2017**, *118*, 106101.

[32] A. Narita, X. Y. Wang, X. Feng, K. Müllen, *Chem. Soc. Rev.* **2015**, *44*, 6616.

[33] Y. Liu, A. Narita, J. Teyssandier, M. Wagner, S. De Feyter, X. Feng, K. Müllen, *J. Am. Chem. Soc.* **2016**, *138*, 15539.

[34] C.-A. Palma, P. Samorì, *Nat. Chem.* **2011**, *3*, 431.

[35] J. Rabe, S. Buchholz, *Science* **1991**, *253*, 424.

[36] J. A. Theobald, N. S. Oxtoby, M. A. Phillips, N. R. Champness, P. H. Beton, *Nature* **2003**, *424*, 1029.

[37] S. Stepanow, M. Lingenfelder, A. Dmitriev, H. Spillmann, E. Delvigne, N. Lin, X. Deng, C. Cai, J. V Barth, K. Kern, *Nat. Mater.* **2004**, *3*, 229.

[38] J. V. Barth, G. Costantini, K. Kern, *Nature* **2005**, *437*, 671.

[39] A. Ciesielski, C. A. Palma, M. Bonini, P. Samorì, *Adv. Mater.* **2010**, *22*, 3506.

[40] C.-A. Palma, M. Cecchini, P. Samorì, *Chem. Soc. Rev.* **2012**, *41*, 3713.

[41] A. Narita, X. Feng, Y. Hernandez, S. a. Jensen, M. Bonn, H. Yang, I. a. Verzhbitskiy, C. Casiraghi, M. R. Hansen, A. H. R. Koch, G. Fytas, O. Ivasenko, B. Li, K. S. Mali, T. Balandina, S. Mahesh, S. De Feyter, K. Müllen, *Nat. Chem.* **2014**, *6*, 126.

[42] J. Lehn, *Chem. Soc. Rev.* **2007**, *36*, 151.

[43] S. De Feyter, F. C. De Schryver, *Chem. Soc. Rev.* **2003**, *32*, 139.

[44] P. Lauffer, K. V. Emtsev, R. Graupner, T. Seyller, L. Ley, *Phys. Status Solidi* **2008**, *245*, 2064.

[45] Q. H. Wang, M. C. Hersam, *Nat. Chem.* **2009**, *1*, 206.

[46] H. Huang, S. Chen, X. Gao, W. Chen, A. T. S. Wee, *ACS Nano* **2009**, *3*, 3431.

[47] S. Barja, M. Garnica, J. J. Hinarejos, A. L. Vázquez de Parga, N. Martín, R. Miranda, *Chem. Commun.* **2010**, *46*, 8198.

[48] H. T. Zhou, J. H. Mao, G. Li, Y. L. Wang, X. L. Feng, S. X. Du, K. Müllen, H. J. Gao, *Appl. Phys. Lett.* **2011**, *99*, 153101.

[49] J. Lu, P. S. E. Yeo, Y. Zheng, Z. Yang, Q. Bao, C. K. Gan, K. P. Loh, *ACS Nano* **2011**, 944.

[50] Q. H. Wang, M. C. Hersam, *Nano Lett.* **2011**, *11*, 589.

[51] J. D. Emery, Q. H. Wang, M. Zarrouati, P. Fenter, M. C. Hersam, M. J. Bedzyk, *Surf. Sci.* **2011**, *605*, 1685.

[52] S. K. Hämäläinen, M. Stepanova, R. Drost, P. Liljeroth, J. Lahtinen, J. Sainio, *J. Phys. Chem. C* **2012**, *116*, 20433.

[53] A. Deshpande, H.-H. Sham, J. M. P. Alaboson, J. M. Mullin, G. C. Schatz, M. C. Hersam, *J. Am. Chem. Soc.* **2012**, *134*, 16759.

[54] H. Zhou, L. Zhang, J. Mao, G. Li, Y. Zhang, Y. Wang, S. Du, W. A. Hofer, H. J. Gao, *Nano Res.* **2013**, *6*, 131.

[55] M. Garnica, D. Stradi, S. Barja, F. Calleja, C. Díaz, M. Alcamí, N. Martín, A. L. Vázquez de Parga, F. Martín, R. Miranda, *Nat. Phys.* **2013**, *9*, 368.

[56] Y. Ogawa, T. Niu, S. L. Wong, M. Tsuji, A. T. S. Wee, W. Chen, H. Ago, *J. Phys. Chem. C* **2013**, *117*, 21849.

[57] H. Yang, A. J. Mayne, G. Comtet, G. Dujardin, Y. Kuk, P. Sonnet, L. Stauffer, S. Nagarajan, A. Gourdon, *Phys. Chem. Chem. Phys.* **2013**, *15*, 4939.

[58] R. Shokri, M. A. Lacour, T. Jarrosson, F. Serein-spirau, K. Miqueu, J. Sotiropoulos, D. Aubel, M. Cranney, G. Reiter, L. Simon, *J. Am. Chem. Soc.* **2013**, *135*, 5693.

[59] P. Järvinen, S. K. Hämäläinen, K. Banerjee, P. Häkkinen, M. Ijäs, A. Harju, P. Liljeroth, *Nano Lett.* **2013**, *13*, 3199.

[60] K. Xiao, W. Deng, J. K. Keum, M. Yoon, I. V. Vlassiouk, K. W. Clark, A. P. Li, I. I. Kravchenko, G. Gu, E. A. Payzant, B. G. Sumpter, S. C. Smith, J. F. Browning, D. B. Geohegan, *J. Am. Chem. Soc.* **2013**, *135*, 3680.

[61] H. J. Karmel, T. Chien, V. Demers-Carpentier, J. J. Garramone, M. C. Hersam, *J. Phys. Chem. Lett.* **2014**, *5*, 270.

[62] A. Riss, S. Wickenburg, L. Z. Tan, H. Z. Tsai, Y. Kim, J. Lu, A. J. Bradley, M. M. Ugeda, K. L. Meaker, K. Watanabe, T. Taniguchi, A. Zettl, F. R. Fischer, S. G. Louie, M. F. Crommie, *ACS Nano* **2014**, *8*, 5395.

[63] J. M. Macleod, F. Rosei, *Small* **2014**, *10*, 1038.

[64] M. N. Nair, C. Mattioli, M. Cranney, J. P. Malval, F. Vonau, D. Aubel, J. L. Bubendorff, A. Gourdon, L. Simon, *J. Phys. Chem. C* **2015**, *119*, 9334.

[65] H.-Z. Tsai, A. A. Omrani, S. Coh, H. Oh, S. Wickenburg, Y. Son, D. Wong, A. Riss, H. S. Jung, G. D. Nguyen, G. F. Rodgers, A. S. Aikawa, T. Taniguchi, K. Watanabe, A. Zettl, S. G. Louie, J. Lu, M. L. Cohen, M. F. Crommie, *ACS Nano* **2015**, *9*, 12168.

[66] K. Banerjee, A. Kumar, F. F. Canova, S. Kezilebieke, A. S. Foster, P. Liljeroth, *J. Phys. Chem. C* **2016**, *120*, 8772.

[67] J. Li, S. Gottardi, L. Solianyk, J. C. Moreno-López, M. Stöhr, *J. Phys. Chem. C* **2016**, *120*, 18093.

[68] M. Gobbi, S. Bonacchi, J. X. Lian, Y. Liu, X.-Y. Wang, M.-A. Stoeckel, M. A. Squillaci, G. D'Avino, A. Narita, K. Müllen, X. Feng, Y. Olivier, D. Beljonne, P. Samorì, E. Orgiu, *Nat. Commun.* **2017**, *8*, 14767.

[69] A. B. Marco, D. Cortizo-Lacalle, I. Perez-Miqueo, G. Valenti, A. Boni, J. Plas, K. Strutyński, S. De Feyter, F. Paolucci, M. Montes, A. N. Khlobystov, M. Melle-Franco, A. Mateo-Alonso, *Angew. Chemie - Int. Ed.* **2017**, *56*, 6946.

[70] F. Liu, W. L. Chow, X. He, P. Hu, S. Zheng, X. Wang, J. Zhou, Q. Fu, W. Fu, P. Yu, Q. Zeng, H. J. Fan, B. K. Tay, C. Kloc, Z. Liu, *Adv. Funct. Mater.* **2015**, *25*, 5865.

[71] S. Vélez, D. Ciudad, J. Island, M. Buscema, O. Txoperena, S. Parui, G. A. Steele, F. Casanova, H. S. J. Van Der Zant, A. Castellanos-Gomez, L. E. Hueso, *Nanoscale* **2015**, *7*, 15442.

[72] D. Jariwala, S. L. Howell, K.-S. Chen, J. Kang, V. K. Sangwan, S. A. Filippone, R. Turrisi, T. J. Marks, L. J. Lauhon, M. C. Hersam, *Nano Lett.* **2016**, *16*, 497.

[73] C. Ojeda-Aristizabal, W. Bao, M. S. Fuhrer, *Phys. Rev. B - Condens. Matter Mater. Phys.* **2013**, *88*, 35435.

[74] H. Hlaing, C.-H. Kim, F. Carta, C.-Y. Nam, R. A. Barton, N. Petrone, J. Hone, I. Kymissis, *Nano Lett.* **2015**, *15*, 69.

[75] S. Parui, L. Pietrobon, D. Ciudad, S. Vélez, X. Sun, F. Casanova, P. Stoliar, L. E. Hueso, *Adv. Funct. Mater.* **2015**, *25*, 2972.

[76] K. Kim, T. H. Lee, E. J. G. Santos, P. S. Jo, A. Salleo, Y. Nishi, Z. Bao, *ACS Nano* **2015**, *9*, 5922.

[77] C. J. Shih, R. Pfattner, Y. C. Chiu, N. Liu, T. Lei, D. Kong, Y. Kim, H. H. Chou, W. G. Bae, Z. Bao, *Nano Lett.* **2015**, *15*, 7587.

[78] T. O. Wehling, K. S. Novoselov, S. V Morozov, E. E. Vdovin, M. I. Katsnelson, A. K. Geim, A. I. Lichtenstein, *Nano Lett.* **2008**, *8*, 173.

[79] H. Liu, Y. Liu, D. Zhu, *J. Mater. Chem.* **2011**, *21*, 3335.

[80] S. Mouri, Y. Miyauchi, K. Matsuda, *Nano Lett.* **2013**, *13*, 5944.

[81] S. Yoshizawa, E. Minamitani, S. Vijayaraghavan, P. Mishra, Y. Takagi, T. Yokoyama, H. Oba, J. Nitta, K. Sakamoto, S. Watanabe, T. Nakayama, T. Uchihashi, *Nano Lett.* **2017**, *17*, 2287.

[82] Viet Phuong Pham, G. Y. Yeom, *Adv. Mater.* **2016**, *28*, 9024.

[83] Q. H. Wang, Z. Jin, K. K. Kim, A. J. Hilmer, G. L. C. Paulus, C. Shih, M. Ham, J. D. Sanchez-yamagishi, K. Watanabe, T. Taniguchi, J. Kong, P. Jarillo-herrero, M. S. Strano, *Nat. Chem.* **2012**, *4*, 724.

[84] G. L. C. Paulus, Q. H. Wang, M. S. Strano, *Acc. Chem. Res.* **2013**, *46*, 160.

[85] M. Amani, D.-H. Lien, D. Kiriya, J. Xiao, A. Azcatl, J. Noh, S. R. Madhvapathy, R. Addou, S. KC, M. Dubey, K. Cho, R. M. Wallace, S.-C. Lee, J.-H. He, J. W. Ager, X. Zhang, E. Yablonovitch, A. Javey, *Science* **2015**, *350*, 1065.

[86] Z. Xia, F. Leonardi, M. Gobbi, Y. Liu, V. Bellani, A. Liscio, A. Kovtun, R. Li, X. Feng, E. Orgiu, P. Samorì, E. Treossi, V. Palermo, *ACS Nano* **2016**, *10*, 7125.

[87] S. Bertolazzi, S. Bonacchi, G. Nan, A. Pershin, D. Beljonne, P. Samorì, *Adv. Mater.* **2017**, *29*, 1606760.

[88] C. A. Di, D. Wei, G. Yu, Y. Liu, Y. Guo, D. Zhu, *Adv. Mater.* **2008**, *20*, 3289.

[89] W. H. Lee, J. Park, S. H. Sim, S. B. Jo, K. S. Kim, B. H. Hong, K. Cho, *Adv. Mater.* **2011**, *23*, 1752.

[90] W. Liu, B. L. Jackson, J. Zhu, C.-Q. Miao, Choon-Heui Chung, Y.-J. Park, K. Sun, J. Woo, Y.-H. Xie, *ACS Nano* **2010**, *4*, 3927.

[91] K. Berke, S. Tongay, M. A. McCarthy, A. G. Rinzler, B. R. Appleton, A. F. Hebard, *J. Phys. Condens. Matter* **2012**, *24*, 255802.

[92] C.-H. Kim, I. Kymissis, *J. Mater. Chem. C* **2017**, *5*, 4598.

[93] D. Lembke, S. Bertolazzi, A. Kis, *Acc. Chem. Res.* **2015**, *48*, 100.

[94] J.-K. Kim, K. Cho, T.-Y. Kim, J. Pak, J. Jang, Y. Song, Y. Kim, B. Y. Choi, S. Chung, W.-K. Hong, T. Lee, *Sci. Rep.* **2016**, *6*, 36775.

[95] J. Dong, F. Liu, F. Wang, J. Wang, M. Li, Y. Wen, L. Wang, G. Wang, J. He, C. Jiang, *Nanoscale* **2017**, *9*, 7519.

[96] H. Yang, J. Heo, S. Park, H. J. Song, D. H. Seo, K. Byun, P. Kim, I. Yoo, H. Chung, K. Kim, *Science* **2012**, *336*, 1140.

[97] W. J. Yu, Z. Li, H. Zhou, Y. Chen, Y. Wang, Y. Huang, X. Duan, *Nat. Mater.* **2012**, *12*, 246.

[98] T. Georgiou, R. Jalil, B. D. Belle, L. Britnell, R. V. Gorbachev, S. V. Morozov, Y.-J. Kim, A. Gholinia, S. J. Haigh, O. Makarovsky, L. Eaves, L. A. Ponomarenko, A. K. Geim, K. S. Novoselov, A. Mishchenko, *Nat. Nanotechnol.* **2012**, *8*, 100.

[99] Y. Choi, J. Kang, D. Jariwala, M. S. Kang, T. J. Marks, M. C. Hersam, J. H. Cho, *Adv. Mater.* **2016**, *28*, 3742.

[100] S. Braun, W. R. Salaneck, M. Fahlman, *Adv. Mater.* **2009**, *21*, 1450.

[101] H. Ma, H.-L. Yip, F. Huang, A. K.-Y. Jen, *Adv. Funct. Mater.* **2010**, *20*, 1371.

[102] M. Gobbi, L. Pietrobon, A. Atxabal, A. Bedoya-Pinto, X. Sun, F. Golmar, R. Llopis, F. Casanova, L. E. Hueso, *Nat. Commun.* **2014**, *5*, 4161.

[103] S. Ryu, L. Liu, S. Berciaud, Y. J. Yu, H. Liu, P. Kim, G. W. Flynn, L. E. Brus, *Nano Lett.* **2010**, *10*, 4944.

[104] Y.-J. Yu, Y. Zhao, S. Ryu, L. E. Brus, K. S. Kim, P. Kim, *Nano Lett.* **2009**, *9*, 3430.

[105] B. J. Kim, E. Hwang, M. S. Kang, J. H. Cho, *Adv. Mater.* **2015**, *27*, 5875.

[106] J. S. Kim, B. J. Kim, Y. J. Choi, M. H. Lee, M. S. Kang, J. H. Cho, *Adv. Mater.* **2016**, 4803.

[107] Y. Zhang, Z. Luo, F. Hu, H. Nan, X. Wang, Z. Ni, J. Xu, Y. Shi, X. Wang, *Nano Res.* **2017**, *10*, 1336.

[108] D. He, Y. Zhang, Q. Wu, R. Xu, H. Nan, J. Liu, J. Yao, Z. Wang, S. Yuan, Y. Li, Y. Shi, J. Wang, Z. Ni, L. He, F. Miao, F. Song, H. Xu, K. Watanabe, T. Taniguchi, J.-B. Xu, X. Wang, *Nat. Commun.* **2014**, *5*, 5162.

[109] W.-T. Hwang, M. Min, H. Jeong, D. Kim, J. Jang, D. Yoo, Y. Jang, J.-W. Kim, J. Yoon, S. Chung, G.-C. Yi, H. Lee, G. Wang, T. Lee, *Nanotechnology* **2016**, *27*, 475201.

[110] H. Sirringhaus, *Adv. Mater.* **2014**, *26*, 1319.

[111] F. Schedin, A. K. Geim, S. V Morozov, E. W. Hill, P. Blake, M. I. Katsnelson, K. S. Novoselov, *Nat. Mater.* **2007**, *6*, 652.

[112] C. Coletti, C. Riedl, D. S. Lee, B. Krauss, L. Patthey, K. von Klitzing, J. H. Smet, U. Starke, *Phys. Rev. B* **2010**, *81*, 235401.

[113] K. K. Kim, A. Reina, Y. Shi, H. Park, L.-J. Li, Y. H. Lee, J. Kong, *Nanotechnology* **2010**, *21*, 285205.

[114] Y. Shi, K. K. Kim, A. Reina, M. Hofmann, L.-J. Li, J. Kong, *ACS Nano* **2010**, *4*, 2689.

[115] C. Christodoulou, A. Giannakopoulos, M. V. Nardi, G. Ligorio, M. Oehzelt, L. Chen, L. Pasquali, M. Timpel, A. Giglia, S. Nannarone, P. Norman, M. Linares, K. Parvez, K. Müllen, D. Beljonne, N. Koch, *J. Phys. Chem. C* **2014**, *118*, 4784.

[116] L. Yang, K. Majumdar, H. Liu, Y. Du, H. Wu, M. Hatzistergos, P. Y. Hung, R. Tieckelmann, W. Tsai, C. Hobbs, P. D. Ye, *Nano Lett.* **2014**, *14*, 6275.

[117] D. H. Kang, J. Shim, S. K. Jang, J. Jeon, M. H. Jeon, G. Y. Yeom, W. S. Jung, Y. H. Jang, S. Lee, J. H. Park, *ACS Nano* **2015**, *9*, 1099.

[118] D. H. Kang, M. S. Kim, J. Shim, J. Jeon, H. Y. Park, W. S. Jung, H. Y. Yu, C. H. Pang, S. Lee, J. H. Park, *Adv. Funct. Mater.* **2015**, *25*, 4219.

[119] V. P. Pham, G. Y. Yeom, *Adv. Mater.* **2016**, *28*, 9024.

[120] D.-H. Kang, M. Hwan Jeon, S. Kyu Jang, W.-Y. Choi, K. Nam Kim, J. Kim, S. Lee, G. Young Yeom, J.-H. Park, *ACS Photonics* **2017**, *4*, 1822.

[121] A. Tarasov, S. Zhang, M.-Y. Tsai, P. M. Campbell, S. Graham, S. Barlow, S. R. Marder, E. M. Vogel, *Adv. Mater.* **2015**, *27*, 1175.

[122] T. O. Wehling, A. I. Lichtenstein, M. I. Katsnelson, *Appl. Phys. Lett.* **2008**, *93*, 202110.

[123] D. Kiriya, M. Tosun, P. Zhao, J. S. Kang, A. Javey, *J. Am. Chem. Soc.* **2014**, *136*, 7853.

[124] W. J. Yu, L. Liao, S. H. Chae, Y. H. Lee, X. Duan, *Nano Lett.* **2011**, *11*, 4759.

[125] E. McCann, *Phys. Status Solidi Basic Res.* **2007**, *244*, 4112.

[126] T. Ohta, A. Bostwick, T. Seyller, K. Horn, E. Rotenberg, *Science* **2006**, *313*, 951.

[127] E. V. Castro, K. S. Novoselov, S. V. Morozov, N. M. R. Peres, J. M. B. L. Dos Santos, J. Nilsson, F. Guinea, A. K. Geim, A. H. C. Neto, *Phys. Rev. Lett.* **2007**, *99*, 216802.

[128] J. B. Oostinga, H. B. Heersche, X. Liu, A. F. Morpurgo, L. M. K. Vandersypen, *Nat. Mater.* **2008**, *7*, 151.

[129] Y. Zhang, T. T. Tang, C. Girit, Z. Hao, M. C. Martin, A. Zettl, M. F. Crommie, Y. R. Shen, F. Wang, *Nature* **2009**, *459*, 820.

[130] F. Xia, D. B. Farmer, Y. Lin, P. Avouris, *Nano Lett.* **2010**, *10*, 715.

[131] T. Taychatanapat, P. Jarillo-Herrero, *Phys. Rev. Lett.* **2010**, *105*, 166601.

[132] M. Sui, G. Chen, L. Ma, W.-Y. Shan, D. Tian, K. Watanabe, T. Taniguchi, X. Jin, W. Yao, D. Xiao, Y. Zhang, *Nat. Phys.* **2015**, *11*, 1027.

[133] Y. Shimazaki, M. Yamamoto, I. V. Borzenets, K. Watanabe, T. Taniguchi, S. Tarucha, *Nat. Phys.* **2015**, *11*, 1032.

[134] A. J. Samuels, J. D. Carey, *ACS Nano* **2013**, *7*, 2790.

[135] J. Park, S. B. Jo, Y.-J. Yu, Y. Kim, J. W. Yang, W. H. Lee, H. H. Kim, B. H. Hong, P. Kim, K. Cho, K. S. Kim, *Adv. Mater.* **2012**, *24*, 407.

[136] X. Zhu, Y. Guo, H. Cheng, J. Dai, X. An, J. Zhao, K. Tian, S. Wei, X. Cheng Zeng, C. Wu, Y. Xie, *Nat. Commun.* **2016**, *7*, 11210.

[137] H. M. D. Bandara, S. C. Burdette, *Chem. Soc. Rev.* **2012**, *41*, 1809.

[138] M. Irie, T. Fukaminato, K. Matsuda, S. Kobatake, *Chem. Rev.* **2014**, *114*, 12174.

[139] R. Klajn, *Chem. Soc. Rev.* **2014**, *43*, 148.

[140] A. Pronschinske, Y. Chen, G. F. Lewis, D. a Shultz, A. Calzolari, M. B. Nardelli, D. B. Dougherty, *Nano Lett.* **2013**, *13*, 1429.

[141] A. Bousseksou, G. Molnár, L. Salmon, W. Nicolazzi, *Chem. Soc. Rev.* **2011**, *40*, 3313.

[142] Kuppusamy Senthil Kumar, M. Ruben, *Coord. Chem. Rev.* **2017**, *346*, 176.

[143] L. Yuan, C. Franco, N. Crivillers, M. Mas-Torrent, L. Cao, C. S. S. Sangeeth, C. Rovira, J. Veciana, C. A. Nijhuis, *Nat. Commun.* **2016**, *7*, 12066.

[144] C. Simão, M. Mas-Torrent, N. Crivillers, V. Lloveras, J. M. Artés, P. Gorostiza, J. Veciana, C. Rovira, *Nat. Chem.* **2011**, *3*, 359.

[145] J. Dugay, M. Aarts, M. Gimenez-Marques, T. Kozlova, H. W. Zandbergen, E. Coronado, H. S. J. Van Der Zant, *Nano Lett.* **2017**, *17*, 186.

[146] M. Giménez-Marqués, M. L. García-Sanz de Larrea, E. Coronado, *J. Mater. Chem. C* **2015**, *3*, 7946.

[147] B. L. Feringa, W. R. Browne, *Molecular Switches*, Wiley-VCH, Weinheim, Germany, **2011**.

[148] M. Kim, N. S. Safron, C. Huang, M. S. Arnold, P. Gopalan, *Nano Lett.* **2012**, *12*, 182.

[149] A. C. Ferrari, J. Robertson, *Phys. Rev. B* **2000**, *61*, 14095.

[150] A. C. Ferrari, D. M. Basko, *Nat. Nanotechnol.* **2013**, *8*, 235.

[151] G. Froehlicher, S. Berciaud, *Phys. Rev. B - Condens. Matter Mater. Phys.* **2015**, *91*, 205413.

[152] A. Jang, E. K. Jeon, D. Kang, G. Kim, B. Kim, D. J. Kang, H. S. Shin, *ACS Nano* **2012**, 9207.

[153] S. Seo, M. Min, S. M. Lee, H. Lee, *Nat. Commun.* **2013**, *4*, 1920.

[154] E. Margapoti, P. Strobel, M. M. Asmar, M. Seifert, J. Li, M. Sachsenhauser, O. Ceylan, C.-A. Palma, J. V. Barth, J. A. Garrido, A. Cattani-Scholz, S. E. Ulloa, J. J. Finley, *Nano Lett.* **2014**, *14*, 6823.

[155] X. Zhang, L. Hou, P. Samorì, *Nat. Commun.* **2016**, *7*, 11118.

[156] J. Li, J. Wierzbowski, Ö. Ceylan, J. Klein, F. Nisic, T. Le Anh, F. Meggendorfer, C. A. Palma, C. Dragonetti, J. V. Barth, J. J. Finley, E. Margapoti, *Appl. Phys. Lett.* **2014**, *105*, 241116.

[157] E. Margapoti, J. Li, Ö. Ceylan, M. Seifert, F. Nisic, T. Le Anh, F. Meggendorfer, C. Dragonetti, C.-A. Palma, J. V Barth, J. J. Finley, *Adv. Mater.* **2015**, *27*, 1426.

[158] S. Wickenburg, J. Lu, J. Lischner, H.-Z. Tsai, A. A. Omrani, A. Riss, C. Karrasch, A. Bradley, H. S. Jung, R. Khajeh, D. Wong, K. Watanabe, T. Taniguchi, A. Zettl, A. H. C. Neto, S. G. Louie, M. F. Crommie, *Nat. Commun.* **2016**, *7*, 13553.

[159] T. Zhang, Z. Cheng, Y. Wang, Z. Li, C. Wang, Y. Li, Y. Fang, *Nano Lett.* **2010**, *10*, 4738.

[160] B. Li, A. V Klekachev, M. Cantoro, C. Huyghebaert, A. Stesmans, I. Asselberghs, S. De Gendt, S. De Feyter, *Nanoscale* **2013**, *5*, 9640.

[161] X. Zhang, E. H. Huisman, M. Gurram, W. R. Browne, B. J. Van Wees, B. L. Feringa, *Small* **2014**, *10*, 1735.

[162] K. S. Mali, J. Greenwood, J. Adisoejoso, R. Phillipson, S. De Feyter, *Nanoscale* **2015**, *7*, 1566.

[163] C. J. Lockhart De La Rosa, R. Phillipson, J. Teyssandier, J. Adisoejoso, Y. Balaji, C. Huyghebaert, I. Radu, M. Heyns, S. De Feyter, S. De Gendt, *Appl. Phys. Lett.* **2016**, *109*, 253112.

[164] S. Cincotti, J. P. Rabe, *Appl. Phys. Lett.* **1993**, *62*, 3531.

[165] Y. J. Zheng, Y. L. Huang, Y. Chen, W. Zhao, G. Eda, C. D. Spataru, W. Zhang, Y. H. Chang, L. J. Li, D. Chi, S. Y. Quek, A. T. S. Wee, *ACS Nano* **2016**, *10*, 2476.

[166] R. Phillipson, C. J. Lockhart de la Rosa, J. Teyssandier, P. Walke, D. Waghray, Y. Fujita, J. Adisoejoso, K. S. Mali, I. Asselberghs, C. Huyghebaert, H. Uji-i, S. De Gendt,

S. De Feyter, *Nanoscale* **2016**, *8*, 20017.

[167] Y. J. Yu, G. H. Lee, J. Il Choi, Y. S. Shim, C. H. Lee, S. J. Kang, S. Lee, K. T. Rim, G. W. Flynn, J. Hone, Y. H. Kim, P. Kim, C. Nuckolls, S. Ahn, *Adv. Mater.* **2017**, *29*, 1603925.

[168] C.-H. Lee, T. Schiros, E. J. G. Santos, B. Kim, K. G. Yager, S. J. Kang, S. Lee, J. Yu, K. Watanabe, T. Taniguchi, J. Hone, E. Kaxiras, C. Nuckolls, P. Kim, *Adv. Mater.* **2014**, *26*, 2812.

[169] S. J. Haigh, A. Gholinia, R. Jalil, S. Romani, L. Britnell, D. C. Elias, K. S. Novoselov, L. A. Ponomarenko, A. K. Geim, R. Gorbachev, *Nat. Mater.* **2012**, *11*, 764.

[170] C.-H. Park, L. Yang, Y.-W. Son, M. Cohen, S. Louie, *Phys. Rev. Lett.* **2008**, *101*, 126804.

[171] C.-H. Park, L. Yang, Y.-W. Son, M. L. Cohen, S. G. Louie, *Nat. Phys.* **2008**, *4*, 213.

[172] S. Dubey, V. Singh, A. K. Bhat, P. Parikh, S. Grover, R. Sensarma, V. Tripathi, K. Sengupta, M. M. Deshmukh, *Nano Lett.* **2013**, *13*, 3990.

[173] M. Rösner, C. Steinke, M. Lorke, C. Gies, F. Jahnke, T. O. Wehling, *Nano Lett.* **2016**, *16*, 2322.

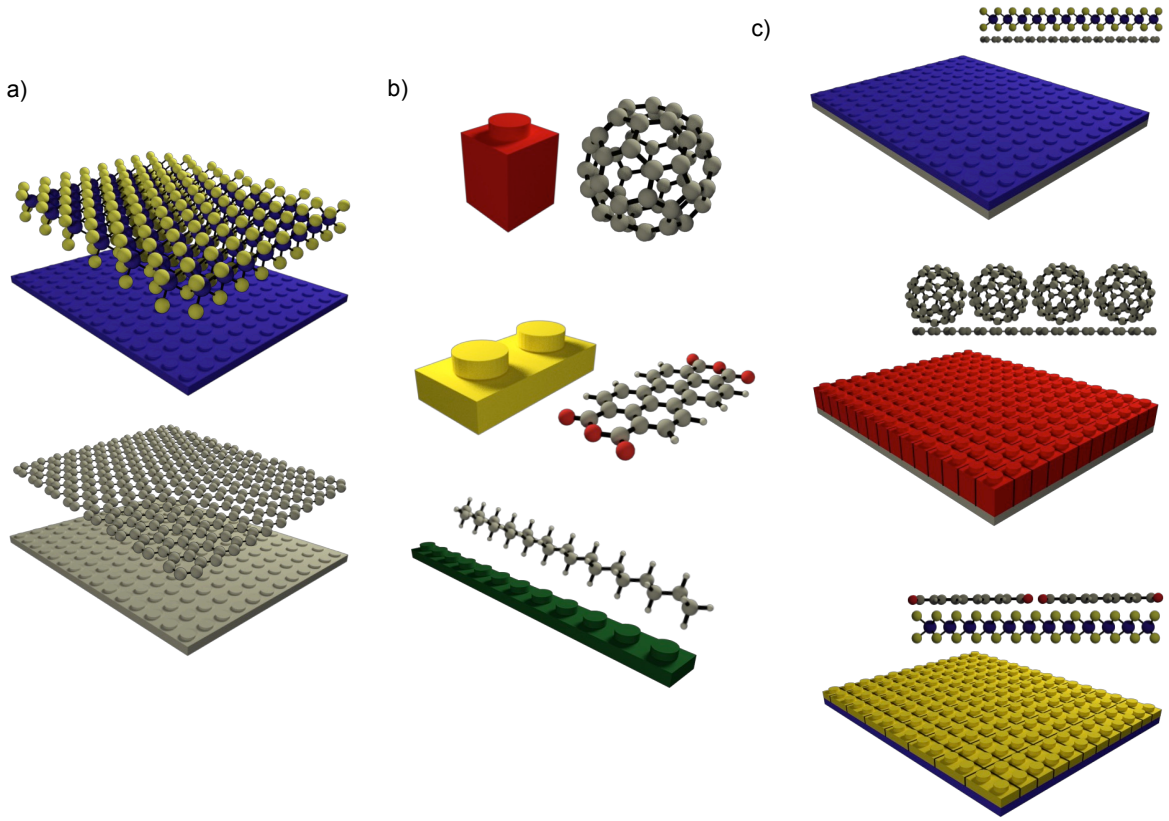

Figure 1. 2D materials obtained from different inorganic layered crystals can be combined to form artificial stacks of materials with on-purpose properties, the so-called van der Waals heterostructures. As such, individual sheets of 2D materials were compared to LEGO planes[12], which can be manipulated and superimposed to obtain more complex structures (a). Following the same analogy, one could consider molecules as smaller LEGO bricks with different shapes and characteristics (b), representing an almost infinite class of diversified materials which can be combined with inorganic 2D sheets to form organic-inorganic structures (c). Importantly, molecules form ordered structures with thickness varying from single layer up to tens-hundreds of nm on 2D materials (c), which can be integrated in vertical stacks. Similarly to the fully inorganic case, the properties of these novel heterostructures are determined by the interactions between individual building blocks and the 2D material.

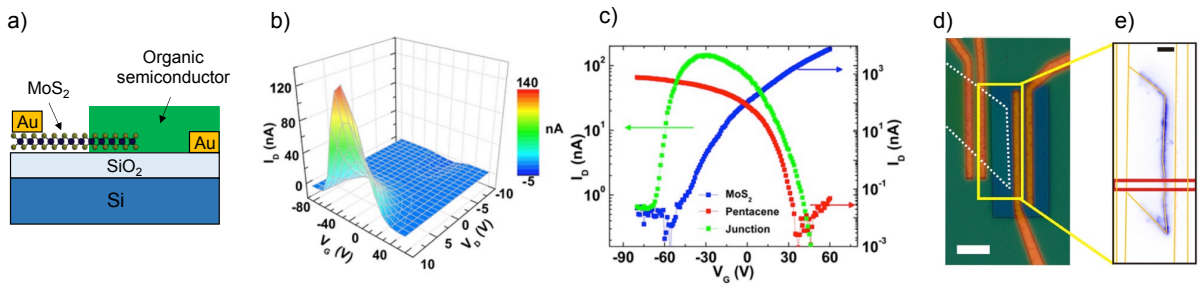

Figure 2. (a) Device architecture of antiambipolar transistors: MoS_2 is used as the n-type region of a p-n heterojunction, while different hole-transporting organic semiconductors act as the p-type region. (b) 3D plot of the transfer curves measured at different applied gate and drain potentials in MoS_2/pentacene devices. Diode-like characteristics are measured only at intermediate gate voltages, so that the device can be considered an anti-ambipolar transistor. (c) Transfer characteristics of the p-n heterojunction compared to those of the separately measured MoS_2 and pentacene layers. (d-e) Optical image of a MoS_2/pentacene device and corresponding photocurrent map. (b-e) Reproduced with permission.[72] Copyright 2016, American Chemical Society.

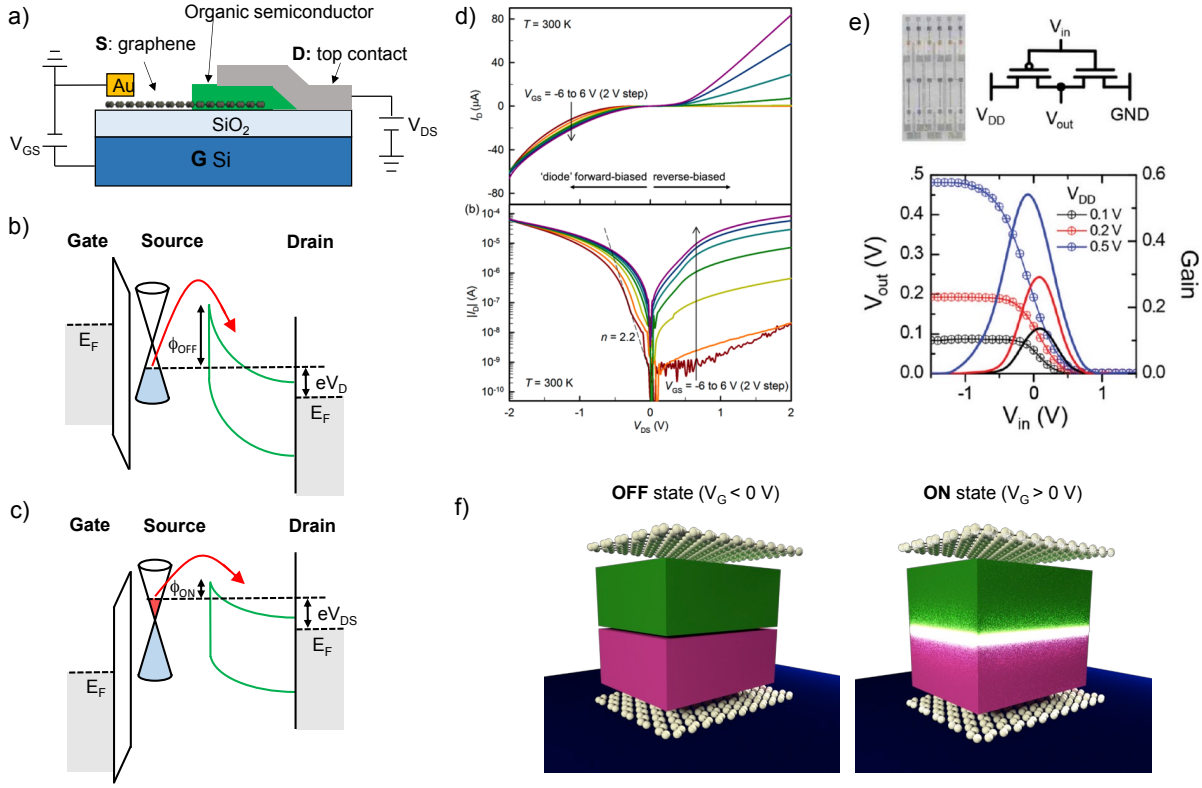

Figure 3: (a) Device architecture of barristors: an organic semiconductor is sandwiched between top metal and bottom graphene electrodes. (b-c) Working mechanism of the graphene-based barristor. The energy barrier for charge injection at the graphene/organic interface is modified by the back gate, resulting in a modulation of the injected current. (d) Gate effect on the I-V characteristics of the vertical transistor (in linear and log scale), as measured for a graphene/C_{60}/Al vertical structure. (e) Complementary inverter fabricated by connecting an n-type and a p-type vertical transistors. (f) A vertical light-emitting transistor could be demonstrated by sandwiching a light-emitting p-n junction between two graphene electrodes with a back-gate. In these conditions, light emission could be switched ON and OFF by a proper gate voltage. (d) Reproduced with permission.[74] Copyright 2015, American Chemical Society. (e) Reproduced with permission.[105] Copyright 2015, WILEY-VCH.

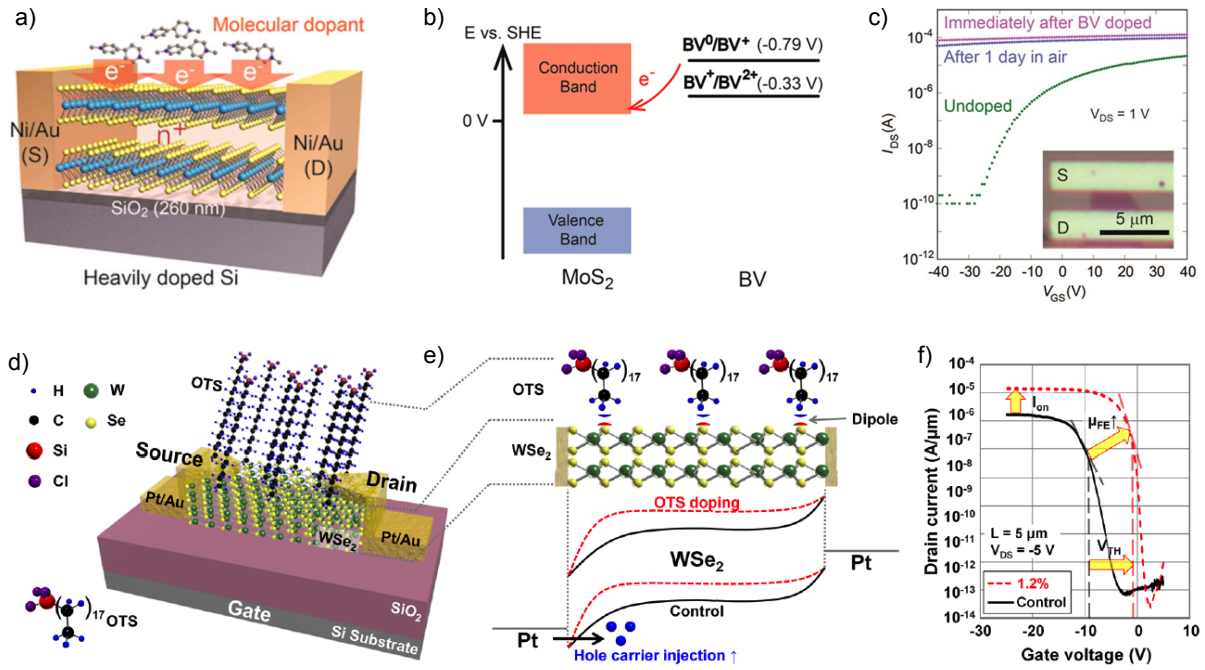

Figure 4: (a) Neutral benzyl viologen molecules are physisorbed on nultilayer MoS_2, inducing charge transfer and n-doping. (b) Energy alignment between the conduction band edge of MoS_2 and the reduction potential of and benzyl viologen. Due to the relative position MoS_2 conduction band and HOMO of the benzyl viologen, electron transfer from the molecule to MoS_2 is energetically favorable. (c) Effect of neutral benzyl viologen molecules onto the electrical characteristics of MoS_2. The sizeable shift of the threshold voltage towards more negative values is indicative of a strong n-type doping. (d) An octadecyltrichlorosilane (OTS) layer introduces p-type doping onto WSe_2, due to aligned molecular dipoles (e), which shift the WSe_2 work function. (f) Effect of the OTS layer onto the electrical characteristics of WSe_2. The shift of the threshold voltage towards more positive values is indicative of moderate p-type doping.(a-c) Reproduced with permission.[123] Copyright 2014, American Chemical Society. (d-f) Reproduced with permission.[117] Copyright 2015, American Chemical Society.

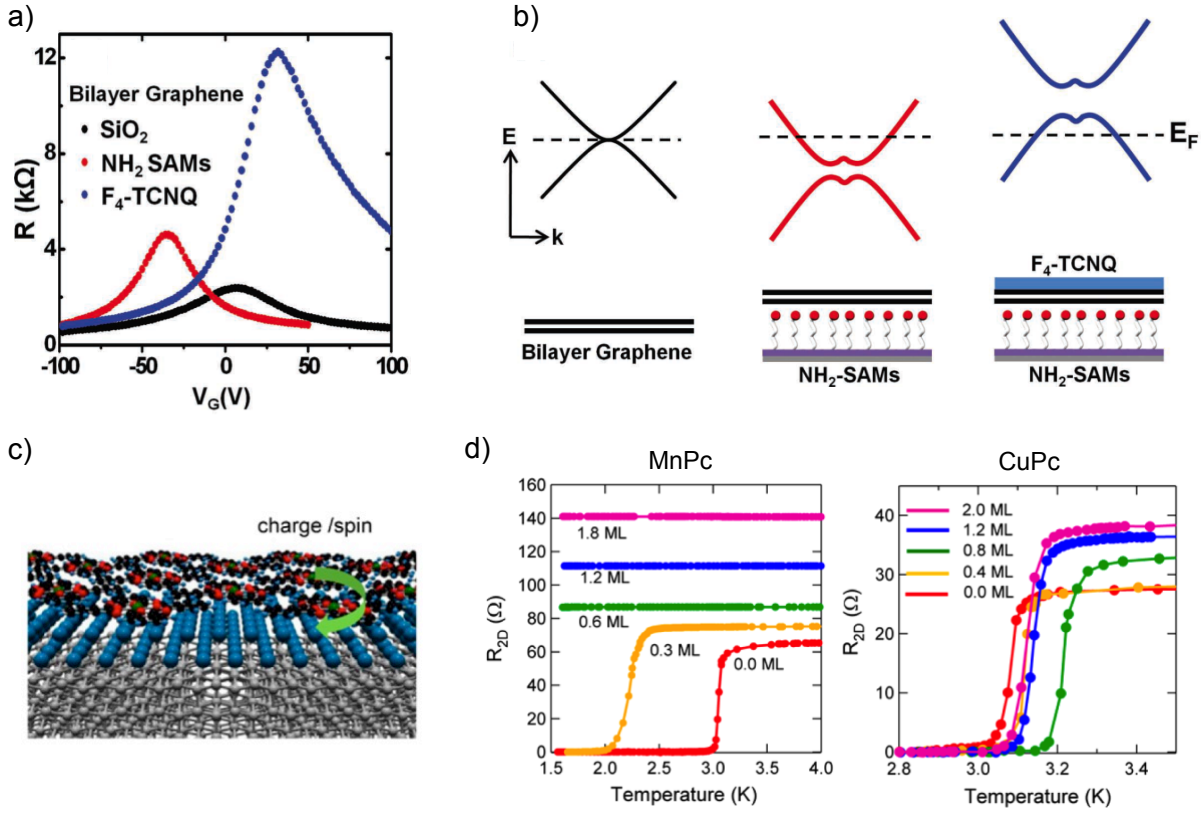

Figure 5: (a) Transfer characteristics of bilayer graphene on SiO_2, on an amino SAM and covered by a F_4TCNQ layer. The I_{ON}-I_{OFF} ratio is increased by the presence of molecules as compared to the pristine case, indicating the opening of a bandgap in the bilayer graphene/organic systems. (b) Molecules introducing significant electric fields across bilayer graphene are effective in opening a bandgap in the latter, by breaking its inversion symmetry. (c) The superconductivity of an In monolayer epitaxially grown on Si is modified by the presence on its surface of two phthalocyanines coordinating different metal ions (Mn, Cu). (d) In the case of MnPc, the superconductivity is largely suppressed, while in the case of CuPc (e) the transition temperature is increased. (a,b) Reproduced with permission.[135] Copyright 2012, WILEY-VCH. (c,d) Reproduced with permission.[81] Copyright 2017, American Chemical Society.

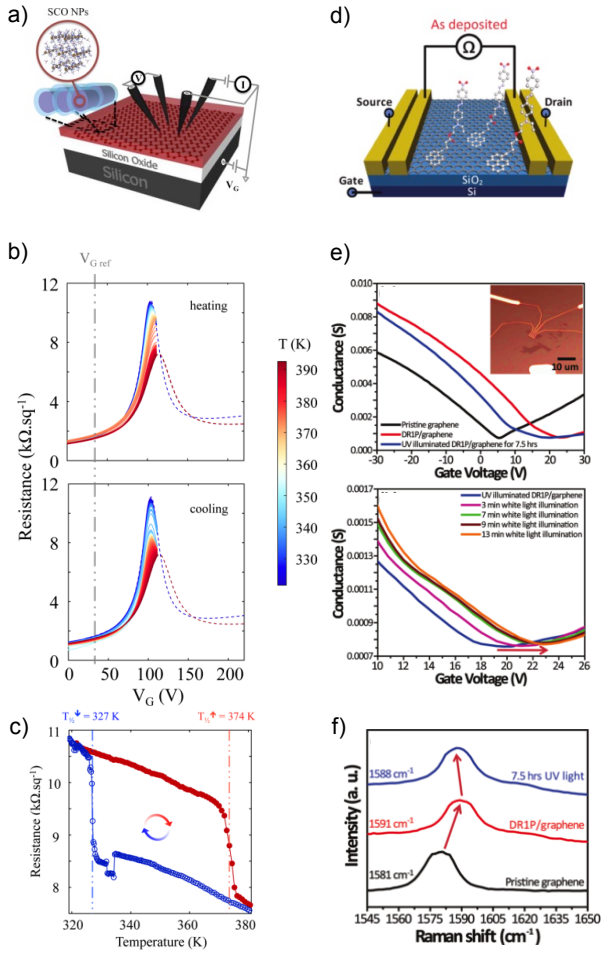

Figure 6: (a) Measurement setup for sensing the molecular spin state in spin crossover (SCO) molecules. A four-probe contact configuration was employed to measure the transfer characteristics of CVD graphene before and after decoration with nanoparticles composed of SCO. (b) Measurement of the electrical characteristics of graphene/SCO system as a function of temperature for heating (top) and cooling (bottom) modes. (c) Temperature dependence of the resistance at the Dirac point, showing a clear hysteresis which follows the SCO switch. (d) Cartoon of the device employed for modulating the graphene conductivity through azobenzene (AZO) photochromic molecules. (e) Electrical characterization of the graphene/AZO bilayers. The I-V trace of the pristine graphene device is shown in black (top panel); after deposition of an AZO film in the trans state, the Dirac point shifts towards

positive values (p-type doping, red trace); after subsequent UV irradiation the Dirac point drifts back towards zero (blue trace). Irradiation with UV light effectively recovers the conductance of the trans state. (f) Raman characterization of the graphene/AZO bilayers. The shift in the G-peak position fully supports the electrical characterization. (a-c) Reproduced with permission.[145] Copyright 2017, American Chemical Society. (d-f) Reproduced with permission.[148] Copyright 2012, American Chemical Society.

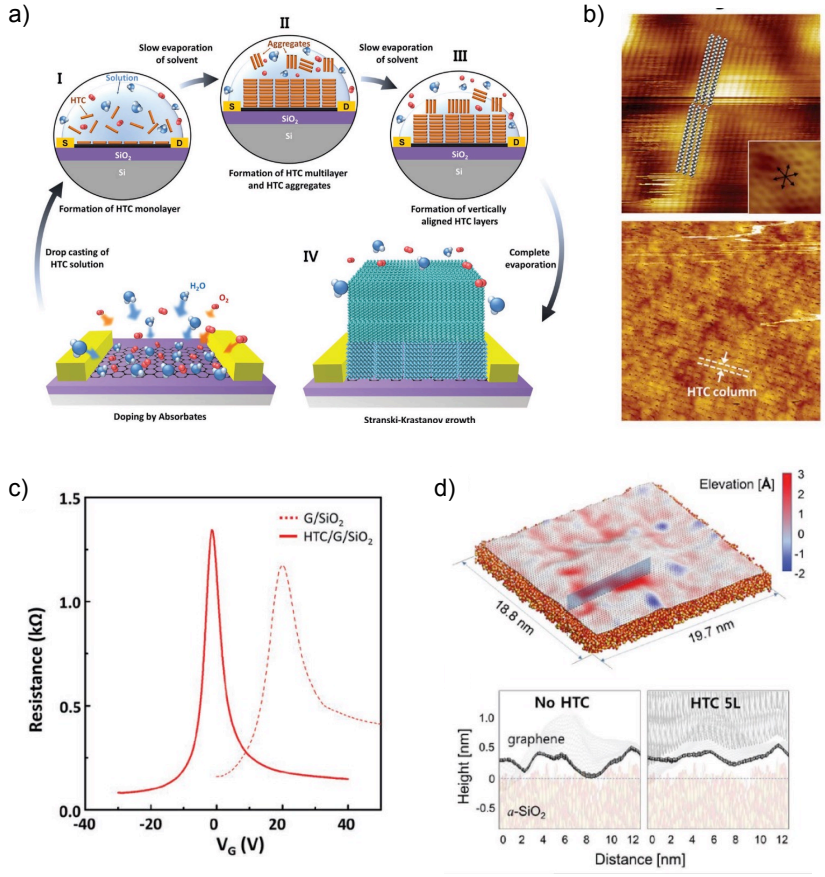

Figure 7: (a) Ordered crystalline structures of the long alkane n-hexatriacontane form on graphene surface by drop-casting and upon slow evaporation of the solvent. (b) STM images of the molecular layer at the initial stage of crystal growth. The alkanes lie flat on graphene, forming a lamellar assembly which follows the roughness of graphene on SiO_2. (c) Transfer characteristics of clean graphene and of the alkane/graphene heterostructure. After the formation of the crystal, the mobility improved and the charge neutrality point was shifted close to zero. (d) Density Functional Theory calculations of the graphene layer roughness before and after formation of the alkane crystal. In the top image, red (blue) corresponds to regions which are lifted (lowered). At the bottom, the calculated profile along the same line before and after the crystal formation is shown. The graphene layer is flattened and lifted from the surface by the presence of the alkane layer. Reproduced with permission.[167]

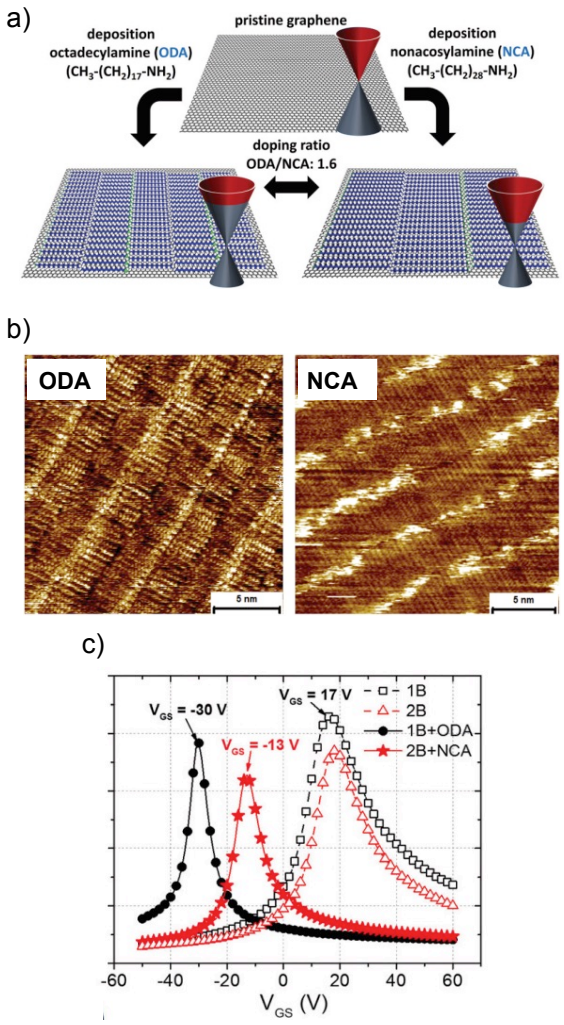

Figure 8: (a) Cartoon of the main idea behind the tunable doping. Molecules composed of a NH_2 dopant group attached to alkyl chains of different lengths were used to introduce controllable doping. The chain length determined the density of dopant groups on the graphene surface, and thus the doping strength. (b) STM images of the assembly of octadecylamine (ODA) and nonacosylamine (NCA), revealing a smaller unit cell in the ODA case, and correspondingly a higher density of dopant heads. (c) Electrical characterization of graphene devices before and after the deposition of an ODA and an NCA layer. In both cases, the charge neutrality point shifted towards more negative values, indicating n-type doping. In excellent agreement with the STM results, the effect was stronger for the ODA case, for

which the density of dopant groups at the surface was higher. Reproduced with permission.

[166] Copyright 2017, Royal Society of Chemistry.

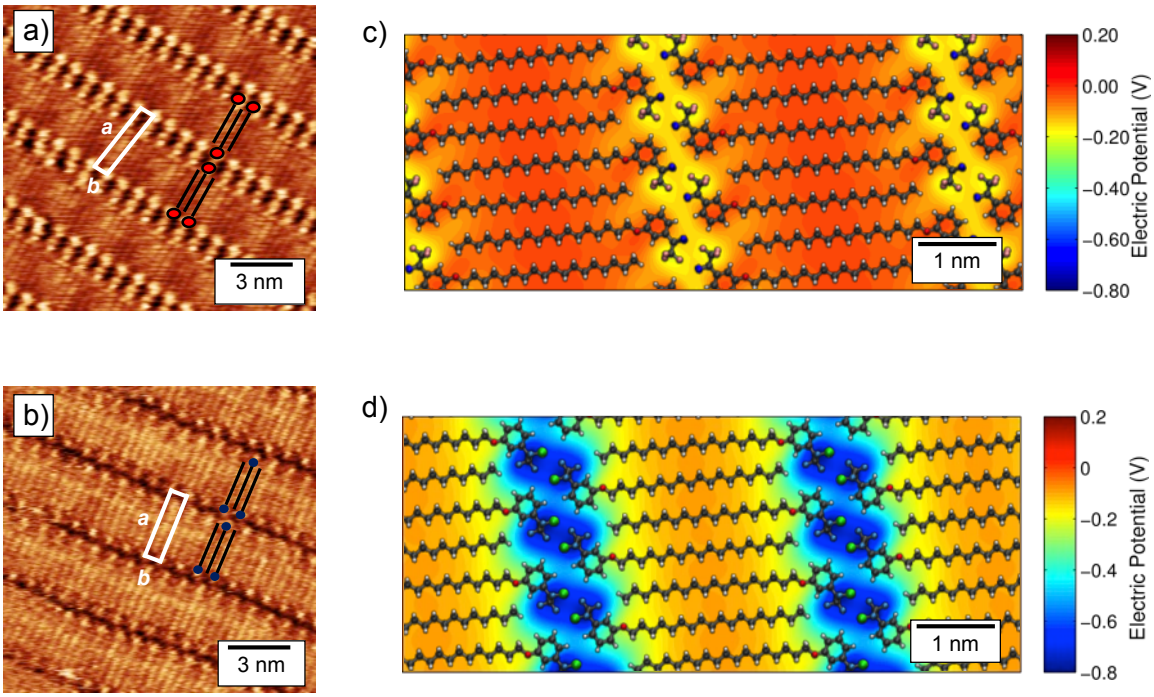

Figure 9: (a) STM image of lamellar self-assembly of the molecule employed in this study, composed of a photoreactive head group and an alkyl chain; (b) STM image of the self-assembly of the molecule reacted under irradiation with UV light in chloroform. While the unit cell extracted by the STM images (a) and (b) was analogous, the doping introduced by the two assemblies onto graphene devices was significantly different. (c-d) Spatial distribution of the electrical potential generated by the molecular dipoles of the unreacted (c) and photolyzed compound (d), calculated on the basis of their nanoscale assemblies. In both cases, the molecular layers introduce a 1D periodic potential, with analogous periodicity (determined by the linear chains) but different amplitude (determined by the graphene/headgroups interaction). Adapted with permission.[68] Copyright 2017, Nature Publishing Group.

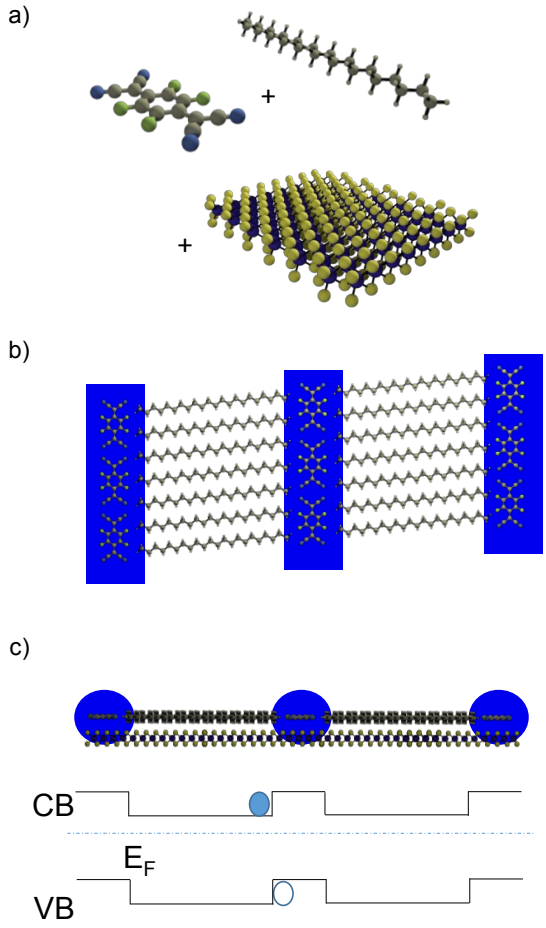

Figure 10: (a) The combination between an n-type 2D semiconductor (MoS_2) with a p-type molecular dopant (F_4TCNQ) and alkanes might lead to a hybrid material with novel properties. (b) Top view of a possible geometry for the co-assembly of F_4TCNQ and alkanes on MoS_2, in which rows of dopants are separated by alkyl chains. In such co-assembly, the p-dopant would induce p-type regions locally (represented as blue areas) separated by the intrinsically n-type MoS_2 below the alkyl chains, and forming a serie of p-n heterojunctions. (c) Side view of the same assembly on MoS_2, with a simplified sketch of the expected modulation in the conduction and valence bands of the latter. The potential introduced by the molecular layer might dramatically change the electronic and optical properties of MoS_2.

((**For Essays, Feature Articles, Progress Reports, and Reviews,** please insert up to three author biographies and photographs here, max. 100 words each))

Marco Gobbi performed his Ph.D in CIC Nanogune in San Sebastian (Spain) and obtained his degree in physics of advanced materials from the University of the Basque Country in 2013. Thereafter he has worked at the Institut de Science et d'Ingénierie Supramoléculaires in Strasbourg (France) and he is currently Marie Curie fellow at the Centro de Física de Materiales, in San Sebastian. Throughout his career, his research activities have focused on the design and fabrication of novel solid state devices in which the electrical performances are determined by an organic/inorganic interface.

Emanuele Orgiu received his M.S. (2004) and Ph.D. (2008) both from Università degli Studi di Cagliari (IT). He was awarded a Fulbright (USA) and Marie-Curie fellowship (FR) in 2007 and 2009, respectively. He became Assistant Professor in 2011 at the Université de Strasbourg (FR) where he was awarded the MIT35 France in 2013. Since 2016, he is also Associate Professor at INRS - EMT Center in Montreal (CA) where, along with his research

team, he focuses on understanding novel electronic and optical phenomena occurring in molecular solids such as organic (semi)conductors or 2D materials such as graphene and transition metal dichalcogenides.

Paolo Samorì is Distinguished Professor and director of the Institut de Science et d'Ingénierie Supramoléculaires of the Université de Strasbourg & CNRS. He is also Fellow of the Royal Society of Chemistry, of the European Academy of Sciences, and of the Academia Europaea, and junior member of the Institut Universitaire de France. After a Laurea in Industrial Chemistry at University of Bologna, he performed his PhD in Chemistry at Humboldt University Berlin. He was also permanent research scientist at CNR of Bologna. His research interests encompass multifunctional 0D to 3D functionalized multicomponent nanostructures and networks thereof for energy, sensing and optoeletronic applications. This includes chemistry of two-dimensional materials (production, tuning of their properties, fabrication of devices). His work was awarded various prizes, including the IUPAC Prize for Young Chemists (2001), the ERC Starting Grant (2010) and the CNRS Silver Medal (2012).